



Originally published as:

Westphal, A., Kleyböcker, A., Jesußeck, A., Lienen, T., Köber, R., Würdemann, H. (2017): Aquifer heat storage: abundance and diversity of the microbial community with acetate at increased temperatures. - *Environmental Earth Sciences*, 76.

DOI: <http://doi.org/10.1007/s12665-016-6356-0>

Aquifer heat storage: abundance and diversity of the microbial community with acetate at increased temperatures

Anke Westphal¹, Anne Kleyböcker¹, Anna Jesuβek², Tobias Lienen¹, Ralf Köber², Hilke Würdemann^{1,3}

¹ GFZ German Research Centre for Geosciences, Section 5.3 Geomicrobiology, 14473 Potsdam, Germany

² Christian-Albrechts-Universität zu Kiel, Institute of Geosciences, 24118 Kiel, Germany

³ Environmental Technology, Water- and Recycling Technology, Department of Engineering and Natural Sciences, Merseburg University of Applied Sciences, 06217 Merseburg, Germany

Abstract

The temperature affects the availability of organic carbon and terminal electron acceptors (TEA) as well as the microbial community composition of the subsurface. To investigate the impact of thermal energy storage on the indigenous microbial communities and the fluid geochemistry, lignite aquifer sediments were flowed through with acetate-enriched water at temperatures of 10 °C, 25 °C, 40 °C, and 70 °C in sediment column experiments. Genetic fingerprinting revealed significant differences in the microbial community compositions with respect to the different temperatures. The highest bacterial diversity was found at 70 °C. Carbon and TEA mass balances showed that the aerobic degradation of organic matter (OM) and sulfate reduction were the primary processes that occurred in all the columns, whereas methanogenesis only played a major role at 25 °C. The methanogenic activity corresponded to the highest abundance of an acetoclastic *Methanosaeta concilii*-like archaeon and the most efficient degradation of acetate. This study suggests a significant impact of geothermal energy storage on the natural microbial community and various metabolic activities because of increased temperatures in sediments with a temperature-related sediment organic matter (SOM) release.

Keywords

Subsurface thermal energy storage, Sediment column experiment, Denaturing gradient gel electrophoresis, Quantitative polymerase chain reaction, Microbial temperature response, Sulfate reduction, Methane production, Carbon use efficiency

Introduction

Underground thermal energy storage in shallow aquifers (aquifer thermal energy storage, ATES, borehole thermal energy storage, BTES) has become an important opportunity to support a sustainable energy supply (Eugster and Sanner 2007, Kabuth et al. this issue). ATES systems are operated at temperature levels below 30 °C (low-temperature [LT-] ATES), between 30 °C to 50 °C (medium-temperature [MT-] ATES) and above 50 °C (high-temperature [HT-] ATES) (Lee 2013). The temperature-induced changes in geochemistry and microbiology of the subsurface have to be investigated to support a site specific evaluation as a basis for a sustainable subsurface planning (Bonte et al. 2011a, Bauer et al. 2013, Hähnlein et al. 2013).

Microorganisms inhabit soils and the shallow subsurface at high densities of 10^4 - 10^6 cells/cm³ (Whitman et al. 1998, Griebler et al. 2002). The subsurface is very heterogeneous and organisms adapt to different natural conditions (Reimann and Garrett 2005). Therefore field evidence of the temperature-related impact is difficult to achieve and the results of *in-situ* investigations are inconsistent (Tab. 1). Hartog et al. (2013) showed distinct microbial communities in different sediments after a similar temperature increase and did not find a significant temperature-related impact in statistical analysis comparing the results of several study sites. However, other *in-situ* studies of shallow ATES and BTES systems revealed an alteration of both the abundance and composition of the microbial community at temperatures between 18 °C and 30 °C (Sowers et al. 2006, Brielmann et al. 2009, Lerm et al. 2011). This was also observed in a 1.3 km deep HT-ATES which assesses a sandstone formation, where besides the temperature, the origin of the fluids and the flow regime also played a major role, influencing the microbial community composition (Lerm et al. 2013, Westphal et al. 2016). Additionally, several laboratory studies showed changes in the microbial community due to temperature increases (Hartog et al. 2013, Bonte et al. 2013a). However, particularly the experimental set-up, such as the sediment and fluid composition, the availability of TEA and organics, the fluid flow velocity as well as the experimental run-time and the sampling intervals influence the microbial abundance and community composition and lead also to differences in the impact of the temperature on the microbial community and therefore make the outcome of studies less comparable (Tab. 1). Furthermore, *in-situ* investigations (Anderson et al. 1973) and laboratory scale column experiments (Gödde et al. 1996) uncovered a correlation between the temperature increase in the soil and the microbial activity. The temperature influences the aquifer ecosystem by altering the solubility of minerals (Arning et al. 2006) as well as by changing the availability of organic matter (OM) and macronutrients (Klein 1989, Brons et al. 1991, Bonte et al. 2011a, b, 2013a, b, Jesušek et al. 2013a) and thus, influencing the biological activity. OM serves as a carbon and/or energy source for microbial metabolism. The efficiency of the organic carbon conversion to microbial biomass (carbon use efficiency, CUE) depends on environmental conditions, such as nutrient availability and temperature (Apple et al. 2006, Allison et al. 2010).

Table 4.1-1. *In-situ* and laboratory scale studies on the influence of temperature on the microbiology in the subsurface due to geothermal energy storage and usage.

	Geothermal installation and purpose	Temperature maximum/ Incubation temperature [°C]	Target Aquifer/ Sediment	Aquifer Depth [m]	Results regarding microbial communities	Location	Reference
<i>In-situ</i> investigations	BTES, Building climatisation	23	Upper and Lower Cohansey	130	Changes in bacterial numbers and types due to temperature increase from 14 °C to 23 °C during ten years of operation	Galloway, New Jersey, USA	Sowers et al. 1997; York et al. 1998; Sowers et al. 2006
	Thermal energy discharge	18	Quarternary Carbonate	15	No changes in bacterial abundance but increased bacterial diversity due to temperatures increase from 11 °C to 18 °C (maximum) No growth of coliforms due to thermal energy discharge	Freising, Germany	Brielmann et al. 2009
	ATES, District heating	30	Quarternary Sands	60	Changes in microbial community composition due different temperatures (7 °C and 20 °C) Operation mode dependent microbial community composition Microbially induced injectivity problems due to iron sulfides and filamentous communities	Berlin, Germany	Lerm et al. 2011a
	ATES, Building climatisation	45	Pleistocene sands	25	Temperature dependence of microbial community (10 °C and 20 °C) Influences on microbial community composition due to operation mode and surface impacts as well as plant construction	Rostock, Germany	Lerm et al. 2011b
	ATES, Research site	28	Coarse Sands	55	Stimulation of faecal bacteria due to temperature increase from 11 °C to 28 °C (maximum)	Eindhoven, Netherlands	Bonte et al. 2011b
	Deep ATES District heating	45, 87	Postera Sandstone	1268	Temperature dependence of microbial diversity and abundance in cold, cooled (45 °C), hot and heated (87 °C) fluids (operation mode) Identification of microbial keyplayers in terms of corrosion and scaling	Neubrandenburg, Germany	Lerm et al. 2013
	ATES, BTES	35, 39	-	-	Quantity and abundance of microorganisms varied within natural variation and were mostly not dependent on temperature More functional variability between than within ATES sites No effect on biodiversity No enrichment of pathogens Reversible community dynamics after ATES abandonment	Netherlands	Hartog et al. 2013
	Deep ATES, District heating	45	Postera Sandstone	1268	Stimulation of sulfur oxidizers due to ingressing oxygen during plant shut down Enrichment of bacteria during stagnant conditions	Neubrandenburg, Germany	Westphal et al. 2016

Table 4.1-1. continued.

Geothermal installation and purpose	Temperature maximum/ Incubation temperature [°C]	Target Aquifer/ Sediment	Aquifer Depth [m]	Results regarding microbial communities	Location	Reference
Laboratory scale experiments	35, 75	Rhine Gravel	-	No enhanced growth of bacteria due to temperature increase to 35 °C and 75 °C Reversible community dynamics No stimulation of pathogens	Germany	Adinolfi et al. 1994
	-20, 8, 20, 30	Bremen Underground	37	No stimulation of bacterial growth due to temperature increase Decreased living cell numbers in sediments incubated at -20 °C	Bremen, Germany	Schippers and Reichling 2006
	4, 10, 15, 20, 30, 45	Quarternary Carbonate	15	No changes in bacterial abundance in sediments due to temperature increase and lowest bacterial diversity at 4 °C and 45 °C Similar sediment community structure between 10 °C and 30 °C Highest microbial cell numbers and microbial diversity at 20 °C in fluids, but no correlation of bacterial diversity with temperature	Freising, Germany	Brielmann et al. 2011
	>80°C	-	-	Shift to mesophilic and thermophilic microbial communities due to temperature increase to temperatures of more than 80 °C	Netherlands	Hartog et al. 2013
	5, 11, 25, 60, 5-80	Pleistocene sands of Sterksel formation	34 36	Different microbial communities in influents and effluents at temperatures above 25 °C Shift in OTUs linked to iron-reducing, sulfate-reducing, methanogenic redox processes due to temperature increase Significant changes in archaeal communities due to temperature increase	Helvoirt, Netherlands Scherpenzeel, Netherlands	Bonte et al. 2013a
	10, 25, 40, 70	Tertiary Lignite Sands	2	Shift from aerobic to iron-reducing, sulfate-reducing, methanogenic and fermentation processes in fluids due to temperature increase Similar metabolic capabilities at each temperature, but temperature dependent microbial community Most efficient conversion of organic matter at 25 °C Highest bacterial diversity at 70 °C Highest CUE at 40 °C Temperature dependent abundance of specific bacterial and archaeal groups	Geesthacht, Germany	This study

Moreover, microbial metabolism and activity can affect the chemical composition of the groundwater, e.g., by altering the redox regime (Jesušek et al. 2013a), and can influence the solid aquifer matrix because of changes in rock porosity and permeability (Chapelle 2000). Studies on drinking water production have shown that biofilm formation and microbially influenced precipitation may lead to the clogging of pores, which leads to the deterioration in well performance (Van Beek 1989, Sand 2003). Therefore, microbial activity can adversely affect the operation of geothermal energy stores. In particular, sulfate-reducing bacteria (SRB) are well-known to be involved in corrosion and scaling processes, and therefore influence technical energy storage installations (Lerm et al. 2013, Westphal et al. 2016, Würdemann et al. 2016). SRB inhabit almost all environments and have functional importance in different ecosystems because of their wide spectrum of TEA, such as sulfate, sulfite, thiosulfate, elemental sulfur, and nitrate (Rabus et al. 2006, Barton and Fauque 2009). The metabolic products of sulfate reduction include several corrosive and toxic sulfur compounds, such as sulfides, bisulfides, and hydrogen sulfide (Videla and Characklis 1992).

The environmental aspects of geothermal energy storage, particularly with regard to the mobilization of soil organic matter (SOM) and the related changes in redox conditions, have rarely been studied. Jesušek et al. (2013a) studied the impact of temperature-related changes in groundwater chemistry in batch and column approaches. Tertiary lignite sand was incubated at four temperatures between 10 °C and 70 °C. The authors observed a shift in the redox regime and a release of sediment organic matter (SOM), ferrous iron, and manganese from the sediment because of the elevated temperatures. Nitrate reduction and reductive iron dissolution occurred at 25 °C, 40 °C, and 70 °C. However, at 10 °C, an incomplete nitrate reduction was found. Sulfate reduction was exclusively initiated at 70 °C. These findings indicated a succession of different microbially catalyzed redox processes that were strongly influenced by a temperature-related SOM release.

To examine the effects of the temperature-induced SOM release on microbial processes, the influent of the long-term column experiments was enriched with acetate (Jesušek et al. 2013b). The authors focused on the redox-reactive degradation of sulfate and the reduction rates at different temperatures. Mole balances for redox reactions were conducted along the flow paths of the columns.

In the study presented here, the microbial community compositions and their effects on OM oxidation at temperatures between 10 °C and 70 °C were studied in the effluents of the experiment presented in Jesušek et al. (2013b) using genetic fingerprinting and quantitative polymerase chain reaction (qPCR). We used mass balances for organic and inorganic carbon and the potential TEA over the entire column to identify the primary microbial metabolic processes in the sediment columns and to correlate these findings with changes in the community composition and the abundance of metabolic groups. With our approach to investigate the effluent water geochemistry, the conversion of OM and TEA as well as the microbial abundance and diversity provide a comprehensive insight into the processes triggered by the temperature increase. We hypothesize that the microbial community composition and abundance in the column effluents reflect the primary processes in the sediment.

Methods

Experimental setup

Four polyethylene tubes measuring 110 cm in length and 10 cm in inner diameter (Fig. 1) were filled with upper lignite sand that was collected one to two meters below the surface from a former gravel pit near Geesthacht. Sediment from the same geological formation was characterized by Hekmat (1982). Only a minor percentage (below 0.1 wt%) of inorganic carbon was detected in the sediment.

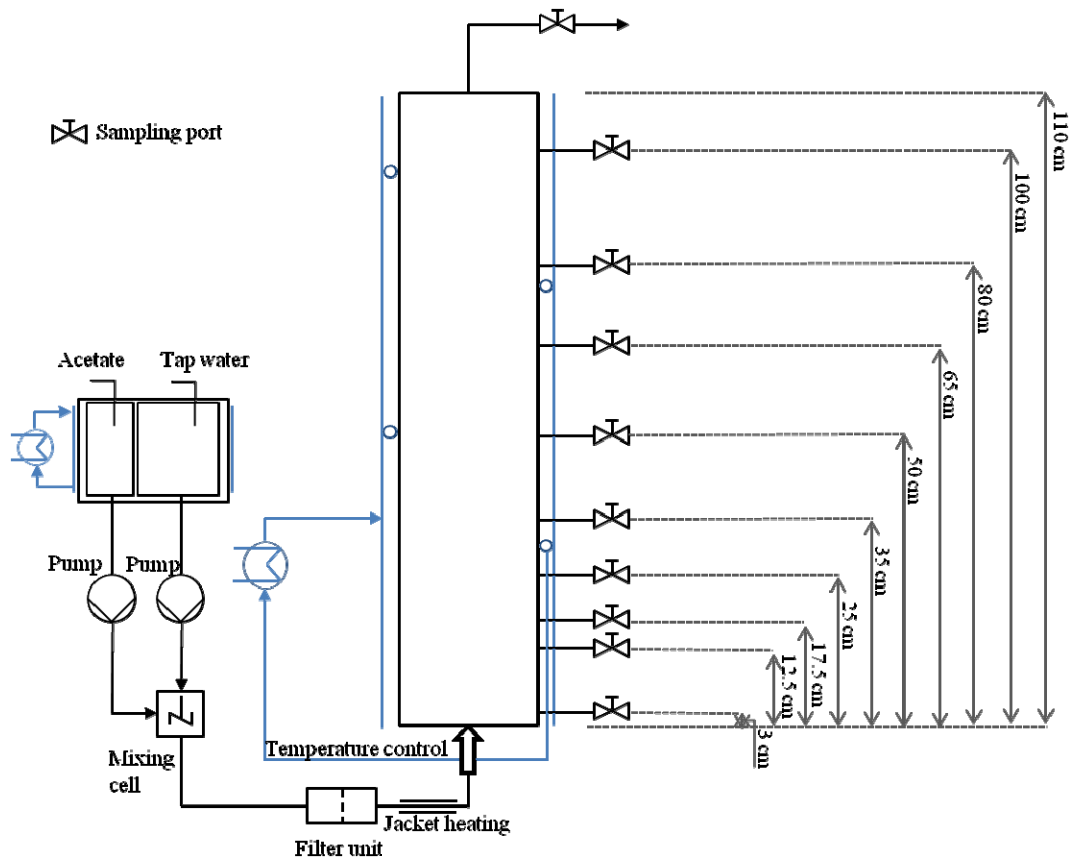


Figure 1. Principal scheme of the sediment columns in the laboratory-scale experiment.

The columns were flowed through by tap water that was produced from an aquifer in the “upper lignite sands” close to Kiel in northern Germany. The pH was 7.47 ± 0.05 . Before column entry, the tap water passed a $0.2 \mu\text{m}$ cellulose acetate filter (2.5 cm in diameter) to prevent the introduction of microorganisms. Sodium acetate was added continuously at a concentration of $18.8 \text{ mg C / L} \pm 1.9 \text{ mg C / L}$ to the tap water as an electron donor substrate for microbial processes to simulate organic carbon release from the sediment. The primary electron acceptors that were continuously introduced with the tap water were oxygen (which was not measured, but amounted approximately to 9.3 mg/L according

to Stadtwerke Kiel 2014), sulfate ($11.8 \text{ mg/L} \pm 1.4 \text{ mg/L}$) and nitrate ($0.62 \text{ mg/L} \pm 0.5 \text{ mg/L}$), whereas manganese and iron were below the detection limit. The average flow rate was 0.9 mL/min . One pore volume exchange (PV) corresponded to 32 hours of column run-time. Each column contained approximately 8.6 dm^3 of sediment. After an adaptation phase at room temperature for 50-70 days, the temperatures of the sediment columns were adjusted to $10 \text{ }^\circ\text{C}$ (reference column, mean groundwater temperature), $25 \text{ }^\circ\text{C}$ (mesophilic column, LT-ATES), $40 \text{ }^\circ\text{C}$ (mesophilic column, MT-ATES), and $70 \text{ }^\circ\text{C}$ (thermophilic column, HT-ATES).

Fluids were collected from nine sampling ports along the flow paths, and were used for chemical analyses. The column effluents were analyzed for the microbial communities after a flow-through of 100 to 285 L.

The column preparation, setup and operation are described in detail in Jesubek et al. (2013a, b).

Sampling for geochemical analyses and water chemistry

For the chemical analyses, 80 mL of fluid were collected from each sampling port. The fluids were analyzed for pH, total inorganic carbon (TIC), total organic carbon (TOC), Ca^{2+} , Mg^{2+} , Na^+ , K^+ , Si_{diss} , Fe^{2+} , Mn^{2+} , CH_3COO^- , CH_4 , NO_3^- , and SO_4^{2-} concentrations. The redox potentials and pH were measured using a pH197i (WTW, Weilheim, Germany). The TIC and TOC were analyzed using a TOC/TN analyzer multi N/C 2000 (Analytik Jena, Jena, Germany). The cation concentrations were determined using an ICP-AES Type Vista AX (Agilent, Santa Clara, USA). The nitrate, sulfate, and acetate concentrations were measured by ion chromatography (IC 881, Metrohm, Switzerland). The methane concentration in the liquid phase was determined by gas chromatography (GC 6890 plus, Headspace HS7694 with molecular sieve packed column, J&W, Agilent, Santa Clara, USA). The detection limits were 0.06 mg/L for nitrate, 0.1 mg/L for sulfate, 0.12 mg/L for acetate, 0.02 mg/L for iron, 0.01 mg/L for manganese and 0.004 mg/L for methane (Jesubek et al. 2013b).

Carbon balances and cumulative curves

Carbon and TEA mass balances were used to identify the prevailing microbial processes at the different temperatures and to assess the plausibility of microbiological findings with respect to the geochemical results. Here, the observed [C]acetate (carbon of acetate) decreases and TIC increases were compared with the calculated microbial [C]acetate consumption and the calculated microbial [C]CO₂ (carbon of CO₂) release, respectively. The formation and dissolution of carbonates were not included because these data could not be determined. However, the pH ranged at 7.5 and the calcium concentration did not change in any of the columns. The cumulative curves were calculated via interpolation according to Eq. 1. It was therefore assumed that the function of the concentration increase in a specific parameter $f(x)$ started at the coordinate origin point.

$$F(x) = \int f(x)dx = \sum_{i=1}^n [(x_i - x_{i-1}) * \frac{f(x_{i-1}) + f(x_i)}{2}]$$

(1)

for $i := \{1, \dots, n\}$ samplings

with $F(x)$ the cumulative increase or decrease of one parameter

$f(x)$ increase or decrease in the concentration of one parameter from the inlet to the outlet of the column

x fluid volume flowed through the column

For the mass balances, the biomass formation, aerobic OM degradation, denitrification, iron reduction, manganese reduction, sulfate reduction, and methane formation were considered (Tab 2). For each microbial process, the corresponding cumulative [C]acetate degradation and cumulative [C]CO₂ release were calculated by the molar ratios of both acetate-carbon and CO₂-carbon to each observed TEA decrease according to the stoichiometric equations in Table 2. The cumulative [C]acetate consumption and [C]CO₂ release caused by the observed [C]methane formation were calculated via the resulting [C]methane according to the equation in Table 2.

Aerobic OM degradation was assumed to take place because the tap water was not de-oxygenated before it was introduced into the columns. The amount of oxygen input was estimated by multiplying the amount of tap water by an oxygen concentration of 9.3 mg/L.

The transfer of organic carbon into biomass was determined according to the CUE values from Table 2. Here, the CUE is defined as the ratio of organic carbon that was fixed in biomass relative to the consumed carbon. For aerobic processes, a CUE value (CUE_{AE}) of 30% was used (Sinsabaugh et al. 2013). For other processes, the CUE values (CUE_{specific}) were calculated by multiplying the CUE_{AE} by the standard free energy yield ratio of the specific process to the aerobic degradation.

Assuming that the sulfide that precipitated with the iron was produced by reductive dissolution, the cumulative acetate consumption and the CO₂ release from iron reduction were calculated. Table 3 gives minimum values for reductive iron dissolution by balancing the iron discharge with the effluent and the maximum value estimated for FeS precipitation together with the effluent discharge of iron.

Table 2: Stoichiometric equations of TEA-consuming processes and methane formation with its standard free energy yields and subsequent specific carbon use efficiency (CUE) values.

Stoichiometric equations of TEA reduction and methane formation	$\Delta G^{0'}$ [kJ/mol_{acetate}]	Reference	CUE_{specific} [%]
$2 \text{O}_2 + \text{CH}_3\text{COO}^- + \text{H}^+ \rightarrow 2 \text{CO}_2 + 2 \text{H}_2\text{O}$	-844	Henze et al. 2013	30
$8\text{NO}_3^- + 5\text{CH}_3\text{COO}^- + 13\text{H}^+ \rightarrow 4\text{N}_2 + 10\text{CO}_2 + 14\text{H}_2\text{O}$	-802	Thauer et al. 1989	29
$4\text{MnO}_2 + \text{CH}_3\text{COO}^- + 2\text{CO}_2 + \text{H}^+ \rightarrow 4\text{Mn}^{2+} + 4\text{CO}_3^{2-} + 4\text{H}_2\text{O}$	-737	Lovely and Philips 1988	26
$8\text{Fe}^{3+} + \text{CH}_3\text{COO}^- + 3\text{H}_2\text{O} \rightarrow 8\text{Fe}^{2+} + \text{HCO}_3^- + \text{CO}_2 + 8\text{H}^+$	-814	Lovely and Philips 1988	29
$\text{SO}_4^{2-} + \text{CH}_3\text{COO}^- + 3\text{H}^+ \rightarrow \text{H}_2\text{S} + 2\text{CO}_2 + 2\text{H}_2\text{O}$	-52	Lovely and Philips 1988	2
$\text{CH}_3\text{COO}^- + \text{H}^+ \rightarrow \text{CH}_4 + \text{CO}_2$	-36	Thauer et al. 1989	1

Sampling and sample preparation for molecular biological analyses

To characterize the microbial community, effluent fluids were collected from the sediment columns at different intervals. Columns running at 25 °C, 40 °C and 70 °C were sampled three times after 220 L to 250 L of flow-through, whereas the 10 °C effluent was sampled once after 110 L of flow-through, given that the column set-up occurred three months later. Samples consisting of 1 L of fluid were collected in sterile Schott Duran glass bottles and transported at a cool temperature of approximately 4 °C until vacuum filtration through cellulose acetate membranes with a 0.2 µm pore size or polycarbonate membrane filters (Sartorius, Göttingen, Germany). After filtration, the filters were stored at -20 °C until further processing.

DNA Extraction

The total DNA was extracted from the filters using the FastDNA™ Spin Kit for Soil (MP Biomedicals, Santa Ana, USA) according to the manufacturer's protocol. The concentration of the extracted DNA was determined fluorimetrically (FLUOstar OPTIMA, BMG Labtech, Ortenberg, Germany) by labeling the DNA with Quant-iT PicoGreen (Invitrogen, Carlsbad, USA).

Table 3: Carbon mass balance: A comparison of the calculated microbial acetate degradation and CO₂ release to the acetate decrease and TIC increase.

(*) The acetate degradation and CO₂ release from iron reduction was calculated on the basis of the observed iron release (□ minimum value). Because this value is underestimated because, e.g., FeS precipitation, the reduced iron that might have precipitated with the H₂S from sulfate reduction was included in the balance as well (□ maximum value).

Comparison of calculated [C]acetate and [C]CO₂ amounts to the corresponding observed amounts								
	[C]acetate	[C]CO ₂	[C]acetate	[C]CO ₂	[C]acetate	[C]CO ₂	[C]acetate	[C]CO ₂
	[mg C]	[mg C]	[mg C]	[mg C]	[mg C]	[mg C]	[mg C]	[mg C]
Calculated carbon amounts resulting from	10 °C	10 °C	25 °C	25 °C	40 °C	40 °C	70 °C	70 °C
biomass formation	193		505		482		451	
aerobic OM degradation	380	380	994	994	958	958	910	910
denitrification	52	52	49	49	47	47	52	52
manganese reduction	12	23	3	6	2	5	1	2
iron reduction*	13	13	13 - 100	13 - 100	10 - 96	10 - 96	1 - 73	1 - 73
sulfate reduction	0	0	694	694	691	691	574	574
methane formation	0	0	356	178	0	0	0	0
Calculated amounts in total	649	468	2615 - 2702	1935 - 2022	2191 - 2277	1711 - 1797	1989 - 2061	1538 - 1610
	[C]acetate	TIC	[C]acetate	TIC	[C]acetate	TIC	[C]acetate	TIC
	[mg C]	[mg C]	[mg C]	[mg C]	[mg C]	[mg C]	[mg C]	[mg C]
Observed amounts	633	401	2353	1696	1210	1277	528	0
Deviation „Calculated“ to „Observed“	3%	14%	10 - 13%	12 - 16%	45 - 47%	25 - 29%	73 - 74%	100%
Flow through amounts	109 L		285 L		275 L		261 L	

Genetic fingerprinting (PCR-DGGE)

Polymerase chain reaction-denaturing gradient gel electrophoresis (PCR-DGGE) was used to characterize the microbial and archaeal community compositions and to detect the changes that occurred among the dominant members of the community.

The fluids were analyzed using DGGE as described by Muyzer et al. (1993). To amplify the partial gene fragments, PCRs were performed using the primer sets 341F-GC/907R for bacterial and 348F-GC/786R for archaeal 16S rRNA as well as 2060F-GC/4R to target the β -subunit of the dissimilatory sulfite reductase (*dsrB*) gene (Tab. 4). The PCR mixtures consisted of 5 μ l of 10x buffer (Genecraft, Cologne, Germany), 1.2 mM dNTPs (Fermentas, Waltham, USA) 3.5 mM MgCl₂ (Genecraft, Cologne, Germany), 0.6 mM of each primer, 0.12 mg/mL BSA, 1.5 u Taq Polymerase (Genecraft, Cologne, Germany) and 1-3 μ L of template DNA. Nuclease-free water was added to a final volume of 50 μ l. The following PCR conditions were used: an initial denaturation at 95 °C for 2:45 min, 30 cycles of 95 °C for 45 s, annealing at primer-specific temperatures (Tab. 4) for 45 s, elongation at 72 °C for 50 s and a final elongation step for 30 min at 72 °C. DGGE was performed using the DCode System (BioRad, Hercules, USA). Equal DNA concentrations of purified PCR products were loaded on polyacrylamide gels with a urea gradient of 35% - 65% for the bacterial and 40% - 70% for the SRB-specific and archaeal analysis. Electrophoresis was run at a constant 115 V and a temperature of 60 °C for 17 h. The resulting bands were excised after silver staining. For reamplification, the same primers were used as those used for the initial PCR, but without a GC clamp at the forward primer. Sequencing was performed by GATC Biotech AG (Konstanz, Germany). The sequences were compared with the sequences in the NCBI database by using the Basic Local Alignment Search Tool (BLAST, NCBI) (Altschul et al. 1990) and with the RDP database by using the Ribosomal Database Project (RDP) Classifier (Wang et al. 2007). The sequences that were analyzed in this study have been deposited in the NCBI database under GenBank accession numbers KT351652 - KT351713.

The Shannon diversity value H' was calculated on the basis of the band abundance and intensity of bacterial and SRB DGGE profiles. The bands and their intensities were scored by GelAnalyzer (gelanalyzer.com). The diversity index was calculated as described in Gafan et al. (2005).

Quantitative PCR

The numbers of gene copies were determined using a SYBR Green real-time PCR approach with the StepOnePlus™ Real-Time PCR System (Applied Biosystems, Carlsbad, USA). To amplify the universal bacterial 16S rRNA fragment, the SRB-specific *dsrA* operon and a specific 16S rRNA fragment of *Methanosaeta*, the primers Uni331F/Uni797R, dsr1F/dsr500R and 585F/855R were used, respectively (Tab. 4). Each PCR reaction contained 10 μ L of Power SYBR Green (Life Technologies), 0.5 μ M of each primer, 10 μ g BSA (Thermo Scientific), and 1 μ L of template DNA. Nuclease-free water (Thermo Scientific) was added to a final volume of 20 μ l. The thermal cycling included an

Table 4: PCR parameters and data of primer pairs used in this study.

Target	Primer Pair	Primer sequence (5'-3')	Product size [bp]	Annealing T[°C]	Reference	Approach
Bacterial 16S rRNA	341F* 907R	CCTACGGGAGGCAGCAG CCGTCAATTCCTTTGAGTTT	560	56	Muyzer et al. 1993 Amann et al. 1992	DGGE
Bacterial 16S rRNA	27F 1492R	AGAGTTTGATCMTGGCTCAG TACGGYTACCTTGTTACGACTT	1460	53	Lane 1991 Lane 1991	qPCR Standard
Bacterial 16S rRNA	331F 797R	TCCTACGGGAGGCAGCAGT GGACTACCAGGGTATCTAATCCTGTT	466	60	Nadkarni et al. 2002 Nadkarni et al. 2002	qPCR
<i>dsrB</i>	2060F* 4R	CCACATCGTYCAYACCCAGGG GTGTAGCAGTTACCGCA	470	55	Geets et al. 2006 Wagner et al. 1998	DGGE
<i>dsrAB</i>	1F 4R	ACSCACTGGAAGCACG GTGTAGCAGTTACCGCA	1905	58	Wagner et al. 1998 Wagner et al. 1998	qPCR Standard
<i>dsrA</i>	1F 500R	ACSCACTGGAAGCACG CGGTGMAGYTCRTCCTG	450	60	Wagner et al. 1998 Wilms et al. 2007	qPCR
Archaeal 16S rRNA	348F* 786R/806R	GYGCAGCAGGCGCGAAA GGACTACVSGGGTATCTAAT	440	60	Sawayama et al. 2004 Takai and Horikoshi 2000	DGGE
<i>Methanosaeta</i> specific 16S rRNA	585F 855R	CCGGCCGGATAAGTCTCTTGA GACAACGGTCGCACCGTGGCC	270	58	Shigematsu et al. 2003 Shigematsu et al. 2003	qPCR Standard qPCR
pGEM-T vector	SP6 T7	ATTTAGGTGACACTATAG TAATACGACTCACTATAGGG	Insert dependent	50	Universal	qPCR Standard
* GC Clamp		CGCCCGCCGCGCCCGCGCCCGTCCCGCCGCCCCGCCCCG			added for DGGE	

initial denaturation step for 10 min at 95 °C followed by 40 cycles of amplification for 10 s at 95 °C, 20 s at respective primer-specific temperatures (Tab. 4) and 30 s at 72 °C. Melting curve analyses were performed. The analyses were performed in triplicates. For the absolute quantification, the full-length bacterial 16S rRNA gene of *Escherichia coli* strain JM109, the *dsrAB* gene of *Desulfotomaculum geothermicum* (DSMZ 3669), and the partial 16S rRNA gene of *Methanosaeta concilii* (DSMZ 6752) were cloned using the pGEM-T Cloning Kit (Promega, Mannheim, Germany). Plasmid dilutions from 10^{-1} to 10^{-8} served as templates for performing qPCR standard curves. The amplification factors were 1.97 for bacterial 16S rRNA, 1.8 for *dsrA*, and 1.84 for the archaeal 16S rRNA approach. The coefficients of determination (R^2) were 0.99, 0.99, and 0.9, respectively. The detection limit of the method was 5×10^2 gene copies per liter for the total bacterial 16S rRNA gene, 2×10^4 gene copies per liter for the *dsr* gene fragments, and 1×10^3 gene copies per liter for the *Methanosaeta*-specific 16S rRNA gene.

Results and Discussion

In the present study, sediment column experiments were used to study the response of the indigenous microbes to increasing temperatures. The effect of SOM release because of temperature increases was enhanced by the addition of acetate as an additional energy and carbon source for microbes.

Shift in the microbial community composition because of temperature increases and degradable organic matter

Significant shifts in the microbial community composition and diversity became obvious due to the temperature increase and the acetate addition. The DNA concentrations were the highest in the 40 °C effluents (2×10^4 ng/L), followed by the 10 °C, 25 °C, and 70 °C effluents (Tab. 5). The DNA concentrations and the total bacterial gene copies in all effluents were similar to those of groundwater wells (McCoy and Olson 1985, Pederson et al. 2008). In our study, bacterial quantification revealed the highest 16S rRNA gene copies/L in the 40 °C effluents, followed by the 25 °C, 10 °C, 70 °C fluids, in descending order (Tab. 5). The gene copy numbers in the 25 °C, 40 °C, and 70 °C effluents remained broadly constant during the 240 L to 275 L flow-through. The gene copy number in the 10 °C effluents after 110 L of flow-through was slightly lower, but still in the same magnitude as in the 25 °C fluids, one magnitude higher than in the 70 °C fluids and one magnitude lower than at 40 °C. Lienen et al. (same issue) also observed the highest bacterial gene copy number in flow-through column experiments with no substrate addition at 40 °C. Brielmann et al. (2011) also observed in the fluids from a laboratory experiment an increase (tripling) in the cell number after the temperature was increased by 10 K above the groundwater temperature.

Table 5: Average total DNA concentrations, eubacterial (EUB) 16S rRNA, SRB-specific *dsrA*, and *Methanosaeta*-specific 16S rRNA gene copies (gc) in the effluent fluids of the 10 °C, 25 °C, 40 °C and 70 °C columns, including the standard deviation (SD). The numbers in light grey refer to values that are near or below the detection limit.

Temperature [°C]	DNA [ng/L]	SD	EUB [gc/L]	SD	SRB [gc/L]	SD	<i>Methanosaeta</i> [gc/L]	SD
10	9x10 ³		3x10 ⁸		2x10 ⁵		6x10 ²	
25	9x10 ³	3x10 ³	4x10 ⁸	2x10 ⁸	4x10 ⁶	2x10 ⁶	1x10 ⁷	5x10 ⁶
40	2x10 ⁴	1x10 ⁴	2x10 ⁹	1x10 ⁹	6x10 ⁷	3x10 ⁷	2x10 ⁴	5x10 ³
70	3x10 ³	3x10 ²	3x10 ⁷	1x10 ⁷	4x10 ⁵	3x10 ⁴	2x10 ³	2x10 ³

In fluids taken from a geothermal borehole well field, cell numbers also increased within the first years of operation at temperatures up to 23 °C and then decreased to numbers similar to those derived from unaffected control sites of 14 °C (York et al. 1998, Sowers et al. 2006). However, in several laboratory studies bacterial numbers in sediments did not increase due to a temperature increase (Schippers et al. 2006, Brielmann et al. 2011). Schippers and Reichling (2006) observed this in a batch approach with no additional substrate supply. Therefore the conditions were very different compared to our approach in which substrates and electron acceptors were supplied continuously. Brielmann et al. (2011) used an extremely high flow velocity of 11 m/d in their column experiments. This led to a retention time of approximately 13 minutes and a 160-times shorter contact time than in our approach with a flow velocity more typical to *in-situ* conditions. Dachroth (2002) showed that flow velocities of 3-5 m/d and above may inhibit biological activity in sandy sediments. Thus, the high fluid flow might have led to a similar bacterial abundance in the column sediments and fluids in the experiments conducted by Brielmann et al. (2011).

Several studies showed that the majority of microorganisms live attached to the sediment in biofilms (Alfreider et al. 1997, Griebler et al. 2002, Brielmann et al. 2011). As biofilm detachment is primarily influenced by shear stress and nutrient availability (Joannis-Cassan et al. 2007), it is assumed that a balance between growth and detachment of mature biofilms established in our long-term experiments that resulted in a continuous discharge of microorganisms as suspension and/or biofilm particles with the effluent (van Loosdrecht et al. 1995, Stoodley et al. 2005) due to an almost constant flow velocity and substrate composition in the influent. Thus, although fluids were collected at the outlet, at a distance of approximately 1 m from the most active zone in the column, the DNA concentrations as well as the bacterial, archaeal and SRB-specific gene copy numbers reflected the community of the active zone. This effect was also observed by Stevenson et al. (2011) who showed that bulk fluid microbial communities represented the structure of biofilm organisms of technical installations from oil production facilities. In addition, geochemical data were in line with the microbiological observations. It is assumed that the oxygen that was introduced with the column inflow solution was

immediately consumed in the first column centimeters and then the conditions turned to anaerobic. Nitrate and sulfate introduced with the influent were also primarily consumed in the nearest zone of the column inlet after a certain adaptation time at all temperatures (Jesuek 2013b) and facultative anaerobic and sulfate reducing microbes were observed in the column effluents.

Genetic fingerprinting analyses revealed distinct microbial communities at the different tempered columns. Similar band patterns were determined for the 25 °C and 40 °C columns, whereas the band patterns at 10 °C and 70 °C showed significant differences. The sequencing of bands revealed the presence of *Betaproteobacteria*, *Clostridia*, and *Bacteroidetes* in 10 °C effluents. However, only *Betaproteobacteria* were identified in the 25 °C effluents. In addition to *Betaproteobacteria*, organisms affiliated to *Gammaproteobacteria*, *Ignavibacteria*, and *Clostridia* were detected in 40 °C effluents. In the 70 °C effluents, most of the sequences were affiliated to *Clostridia* as well as to *Bacilli*, *Betaproteobacteria*, and *Bacteroidia* (Tab. 6). In addition, an adaptation at DNA level to thermophilic conditions became obvious as the bands in the 70 °C lane migrated furthest into the gel bottom, due to a higher guanine-cytosine (GC) content within the gene fragment indicating a temperature stabilization of the DNA at 70 °C

The temperature increase to 70 °C led to a significant change in the microbial community dominated by thermotolerant and thermophilic bacteria that are commonly isolated from soils, aquifers, geothermal waters, and hot springs (Mori et al. 2002, Zavarina et al. 2002, Poli et al. 2006, Ogg and Patel 2009, Fardeau et al. 2010). The high diversity of fermenting bacteria reflected the SOM release at 70 °C. The adaptation from psychrophilic to mesophilic and thermophilic microbial communities was also shown by Hartog et al. (2013) and Bonte et al. (2013a), who heated different aquifer sediments to temperatures of up to 80 °C. Similar observations were also performed by Isaksen et al. (1994), who detected thermophilic SRB and fermentative bacteria in cold marine sediments that were heated to a maximum temperature of 80 °C. An adaption of the microbial community composition to increased temperatures, was also determined in several field and laboratory studies (Sowers et al. 2006, Brielmann et al. 2009, Lerm et al. 2011a, Lerm et al. 2013, Lienen et al. same issue). Remarkably, also Brielmann et al. (2011) found a similar community structure in the mesophilic temperature range (Fig. 2A). The microbial biocenosis was stimulated by the acetate addition that triggered the initiation of sulfate reduction (Jesuek et al. 2013b). In addition, the temperature increase and the acetate addition led to an increase in the microbial diversity in the effluents. The Shannon diversity value was the lowest for the 10 °C effluents, at 2.8. For the 25 °C and 40 °C effluents, the Shannon diversity was the same, at 3.1. The highest Shannon diversity was observed in the 70 °C effluents with 3.5. This is in contrast to other studies focusing on microbial communities in temperature-affected groundwater environments. Field studies by Brielmann et al. (2009) showed the highest bacterial diversity at the maximum temperature of 18 °C. In addition, when incubating quaternary sediments at 20 °C, Brielmann et al. (2011) observed a microbial diversity increase in fluids and a slightly decreased diversity at 45 °C. Bonte et al. (2013a) observed the highest diversity at

Table 6: Phylogenetic affiliation of partial bacterial 16S rRNA gene sequences from DGGE profiles of fluid samples that were collected at the outlet of the four different tempered sediment columns. Taxonomic assignments were performed by RDP Classifier with a confidence threshold of 80%. For each phylotype, the most closely related sequence and the closest cultivated organism are given, including GenBank accession numbers.

T[°C]	Band No.	Closest phylotype (accession no.)	BLAST similarity (%)	Closest described relative (accession no.)	BLAST similarity (%)	Taxonomic classification	Genbank accession no.
	1	Uncultured bacterium (JX120472)	91	<i>Thauera</i> sp. (AM084110)	91	Unclassified Rhodocyclaceae	KT351652
	2	Uncultured bacterium (FQ659581)	99	<i>Prolixibacter bellariivorans</i> (AB541983)	91	<i>Prolixibacter</i>	KT351653
10	3-5	Uncultured bacterium (KF641316)	97	<i>Desulfosporosinus</i> sp. (JX412369)	97-99	<i>Desulfosporosinus</i>	KT351654 -6
	6			<i>Dechloromonas</i> sp. (AB769215)	96	Unclassified Rhodocyclaceae	KT351657
	7	Uncultured bacterium (JX222991)	100	<i>Thauera</i> sp. (AM084110)	100	<i>Zoogloea</i>	KT351658
	8,9			<i>Azospira</i> sp. (GU202937)	98, 99	<i>Azospira</i>	KT351659 -60
	10			Bacterium (JQ765451)	77	Unclassified Bacteria	KT351661
25	11-16	Uncultured bacterium (KF493720)	95-100	<i>Azospira</i> sp. (KC247691)	97-100	<i>Azospira</i>	KT351662 -7
	17	Uncultured <i>Ferribacterium</i> (AB849300)	99	<i>Ferribacterium</i> sp. (HM124374)	99	<i>Ferribacterium</i>	KT351668
	18,19			<i>Aquabacterium</i> sp. (KC424519)	98,99	Unclassified Burkholderiales	KT351669 -70
	20	Bacterium enrichment culture (JF449928)	94	<i>Melioribacter roseus</i> (NR_074796)	90	Unclassified Bacteria	KT351671
	21-23	Uncultured bacterium (KF493720)	94-100	<i>Azospira</i> sp. (KC247691)	94-100	<i>Azospira</i>	KT351672 -4
40	24			<i>Azospira</i> sp. (GU202937)	99	<i>Azospira</i>	KT351675
	25	Uncultured bacterium (GQ480082)	97	<i>Zoogloea</i> sp. (KC473458)	96	<i>Zoogloea</i>	KT351676
	26			<i>Lysobacter</i> sp. (JN848797)	92	Unclassified Proteobacteria	KT351677
	27	Uncultured <i>Clostridia</i> bacterium (EU522656)	99	<i>Desulfotomaculum</i> sp. (AJ577273)	93	Unclassified Peptococcaceae	KT351678
	28			<i>Aquabacterium</i> sp. (KC424519)	100	<i>Aquabacterium</i>	KT351679
	29	Uncultured <i>Clostridia</i> bacterium (DQ208699)	92	<i>Thermanaeromonas toyohensis</i> (NR_024777)	91	<i>Thermanaeromonas</i>	KT351680
	30	Uncultured bacterium (KC736337)	99	<i>Anoxybacillus amylolyticus</i> (NR_042225)	99	<i>Anoxybacillus</i>	KT351681
	31	Uncultured bacterium (EU160525)	99	<i>Thermicanus aegyptius</i> (NR_025355)	98	<i>Thermicanus</i>	KT351682
	32	Uncultured bacterium (GQ045714)	81	<i>Acetomicrobium</i> sp. (JQ707908)	81	Unclassified Bacteria	KT351683
	33			<i>Thermanaeromonas toyohensis</i> (NR_024777)	98	<i>Thermanaeromonas</i>	KT351684
70	34			<i>Desulfurispora thermophila</i> (NR_042969)	86	<i>Desulfurispora</i>	KT351685
	35	Uncultured bacterium (FR846903)	97	<i>Sideroxydans lithotrophicus</i> (NR_074731)	93	Unclassified Rhodocyclaceae	KT351686
	36			<i>Desulfotomaculum salinum</i> (AY918123)	96	Unclassified <i>Clostridia</i>	KT351687
37, 38		Uncultured low G+C Gram-positive bacterium (AF027087)	96, 97	<i>Clostridium</i> sp. (FJ808611)	90	Unclassified Firmicutes	KT351688 -9
	39			<i>Fervidicola ferrireducens</i> (NR_044504)	98	<i>Fervidicola</i>	KT351690
	40	Uncultured bacterium (AY862531)	93	<i>Thermovenabulum ferriorganovorium</i> (NR_042719)	85	Unclassified Bacteria	KT351691
	41			<i>Clostridiales</i> bacterium (GQ405534)	81	Unclassified Bacteria	KT351692

25 °C in sediment column experiments and a decrease in the microbial diversity following a further temperature increase to 60 °C. The lower diversity at higher temperatures might be related to the shorter adaptation time of 25 days or to a lower availability of organic substrates as energy and carbon source.

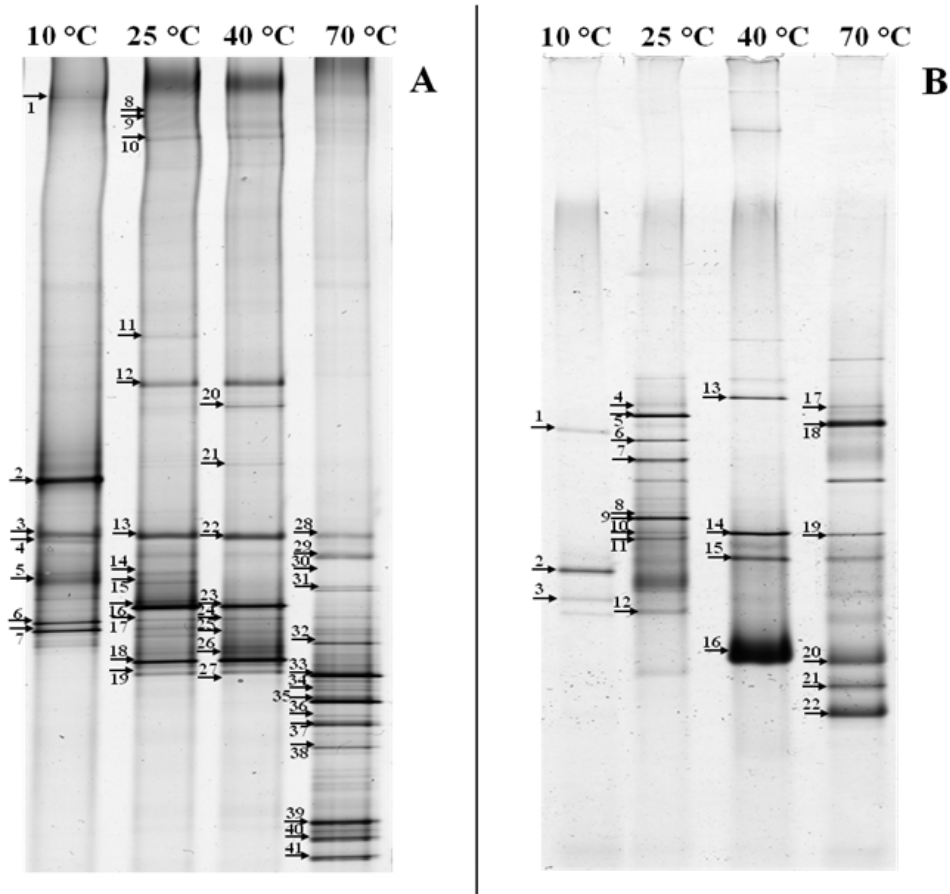


Figure 2. Genetic fingerprinting of PCR-amplified bacterial 16S rRNA fragments (A) and *dsrB* genes (B) from fluids collected at the outlets of the 10 °C, 25 °C, 40 °C, and 70 °C columns. Because the banding pattern did not change over the time of investigation, one representative profile is shown for each temperature. Numbered arrows indicate the sequenced bands.

Changes in SRB diversity, abundance, and activity due to a temperature increase and degradable organic matter

Specific fingerprinting analyses based on *dsrB* and *dsrA* gene fragments also showed a shift in the SRB community in response to the temperature increase and the acetate addition (Fig. 2B). SRB-specific genetic fingerprinting revealed additional SRB representatives in all the effluents, besides the already detected species of *Desulfosporosinus* (10 °C), *Desulfotomaculum* (25 °C, 40 °C, 70 °C), and *Desulfurispora* (70 °C). In the 10 °C effluent, sequences affiliated with uncultured *Thermosinus* sp. were detected in addition to those of *Desulfotomaculum* sp.. However, in the 25 °C, 40 °C, and 70 °C

effluents, the sequences were assigned to *Desulfosporosinus* and *Desulfotomaculum*. Mesophilic and thermophilic *Desulfosporosinus* and *Desulfotomaculum* species are frequently found in subsurface environments (Campbell and Postgate 1965, Daumas et al. 1988, Stackebrandt et al. 1997, Geets et al. 2005, Parshina et al. 2005). Relatives of the mesophilic *Desulfovibrio fructosovorans* (Ollivier et al. 1988) were also detected in the 25 °C effluents and sulfate reducers related to *Syntrophobacter fumaroxidans* were only found at 40 °C and 70 °C (Tab. 7).

In the 25 °C effluents, the highest Shannon diversity index of SRB was observed with 2.8, followed by the other temperatures, for which the index ranged between 2.2 and 2.4. An adaptation of the SRB community to increased temperatures was observed, among others, by Robador et al. (2009), Hubert et al. (2009), Bonte et al. (2013a), and de Rezende et al. (2013).

In relation to the main TEA, oxygen and sulfate, that were introduced with the influent acetate was fed in excess with a factor between two and three (Jesušek et al. 2013b). The acetate concentration consistently decreased with the sulfate concentration along the flow paths (Fig. 3). At 10 °C, 40 °C, and 70 °C, the acetate concentration decreased between 17% and 25% within the first 13 cm of the column and then remained constant after 110 L, 195 L, and 195 L of flow-through. However, at 25 °C, methane was formed acetoclastically by *M. concilii* at sulfate concentration below 4.8 mg/L and led to an acetate decrease below the detection limit. At 10 °C, sulfate reduction was initiated after a flow-through of 110 L and that went along with a further decrease in acetate. At 25 °C, 40 °C, and 70 °C, the sulfate reduction was already initiated after 58 L, 21 L, and 1.3 L of flow-through, respectively, and it decreased rapidly (Jesušek et al. 2013b). The distance from the fluid inlet to the initiation of sulfate reduction shifted towards the column inlet with increasing flow-through. When the sulfate reduction ran, the sulfate concentration along the flow path decreased from the introduced 11.8 mg/L to sulfate concentrations below 3.3 mg/L at 10 °C and close to the detection limit (0.3 mg/L) in the 25 °C and 40 °C fluids. In the 70 °C column, the sulfate concentration decreased to 1.4 mg/L at the same distance.

The concurrent decrease of acetate and sulfate in the sediment columns as well as the detection of SRB and the consistence of the mass balances indicated that acetate was used by the SRB to reduce the sulfate. This finding is in accordance with Sørensen et al. (1981) who concluded that acetate is a major substrate for SRB. Within the diverse SRB group, several species are known to oxidize different organic substrates and also to convert acetate into CO₂ (Sørensen et al. 1981, Parkes et al. 1989, Rabus 2006). For example, species related to *Desulfotomaculum* and *Desulfovibrio* have the ability to use acetate as a carbon source (Widdel and Pfennig 1977, 1981, 1984, Widdel 1980, Pfennig et al. 1981). In the 25 °C and 40 °C effluents, the sulfate concentrations decreased to values close to the detection limit. However, in the 70 °C effluents, the primary decrease in the acetate concentration went along with a lower decrease in the sulfate concentration. This finding indicated that additional processes occurred under thermophilic conditions. Trapped gases in the sediment columns shortened the residence time and formed stagnation zones, which were not supplied with electron acceptors by the

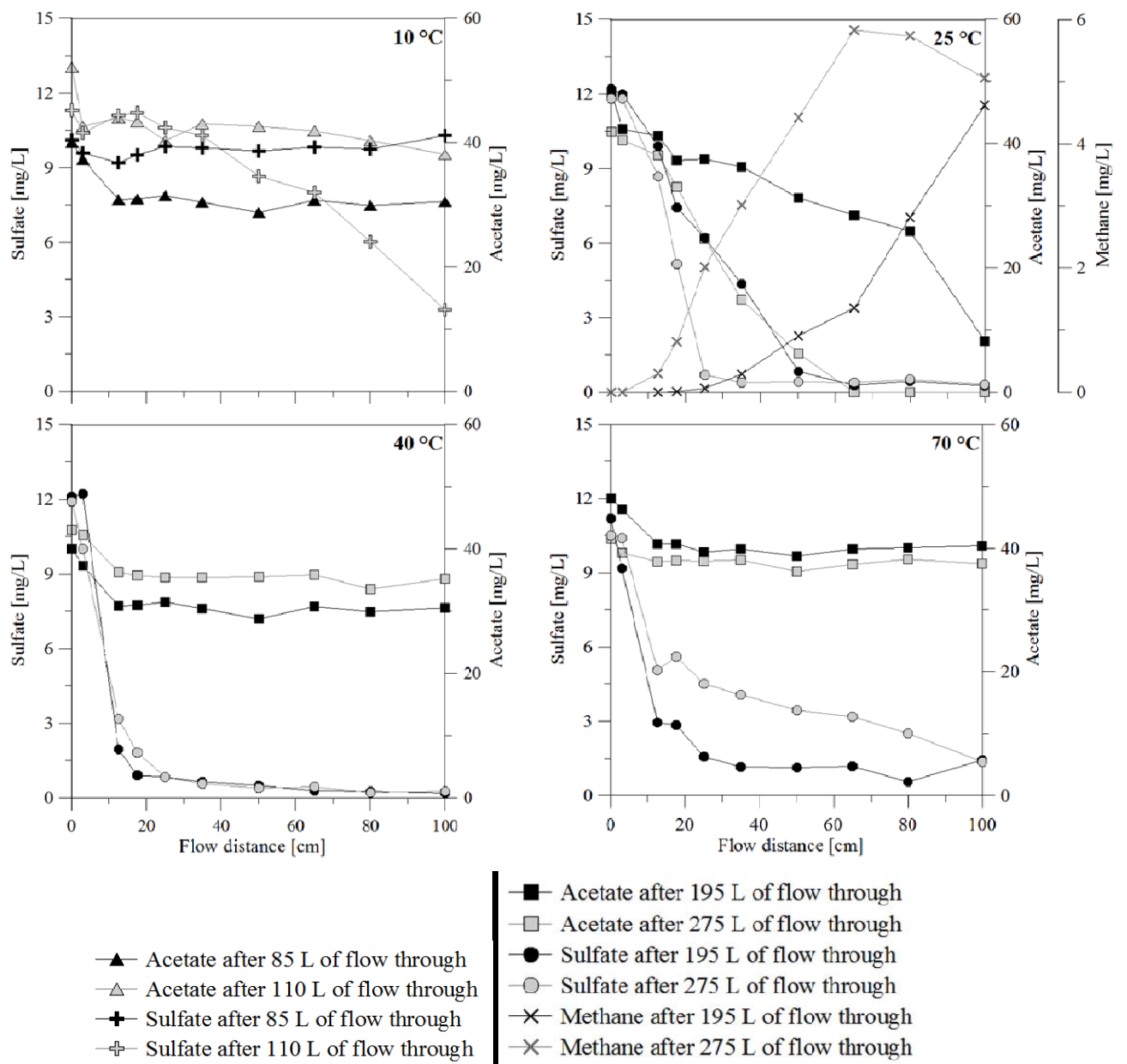


Figure 3. Sulfate, acetate and methane concentrations dependent on the residence time indicated as the flow distance in cm in the 10 °C, 25 °C, 40 °C, and 70 °C columns after certain times of flow through with respect to times of molecular biological sampling.

Table 7. Phylogenetic affiliation of partial *dsrB* gene sequences from DGGE profiles of fluid samples that were collected at the outlet of the four different tempered sediment columns. For each phylotype, the most closely related sequence and the closest cultivated organism are given, including GenBank accession numbers.

T[°C]	Band No.	Closest phylotype (accession no.)	BLAST similarity (%)	Closest cultivated relative (accession no.)	BLAST similarity (%)	Genbank accession no.
10	1	Uncultured sulfate-reducing bacterium (AY251458)	95	<i>Desulfotomaculum carboxydans</i> (CP002736)	78	KT351693
	2	Uncultured <i>Thermosinus</i> sp. (FJ648439)	94			KT351694
	3	Uncultured <i>Thermosinus</i> sp. (FJ648439)	98			KT351695
25	4, 5	Uncultured sulfate-reducing bacterium (AB610179)	94			KT351696 - 7
	6	Uncultured bacterium (FJ948567)	89	<i>Desulfosporosinus</i> sp. (AY787791)	86	KT351698
	7	Uncultured bacterium (HQ690808)	90			KT351699
	8	Uncultured sulfate-reducing bacterium (AB610179)	87	<i>Desulfotomaculum runinis</i> (CP002780)	76	KT351700
	9	Uncultured prokaryote (JN615163)	89			KT351701
	10	Uncultured prokaryote (JN615166)	79			KT351702
	11	Uncultured sulfate-reducing bacterium (DQ855254)	78	<i>Desulfovibrio fructosivorans</i> (AF418187)	76	KT351703
	12	Uncultured <i>Thermosinus</i> sp. (FJ648439)	90	<i>Desulfovibrio fructosivorans</i> (AF418187)	78	KT351704
40	13	Uncultured <i>Desulfotomaculum</i> sp. (DQ415722)	93	<i>Desulfotomaculum geothermicum</i> (AF273029)	89	KT351705
	14	Uncultured sulfate-reducing bacterium (KC865378)	79	<i>Syntrophobacter fumaroxidans</i> (CP000478)	79	KT351706
	15, 16	Uncultured bacterium (FJ948567)	91	<i>Desulfosporosinus</i> sp. (AY787791)	88, 89	KT351707 - 8
70	17	Uncultured sulfate-reducing bacterium (HQ148570)	78	<i>Syntrophobacter fumaroxidans</i> (CP000478)	89	KT351709
	18	Uncultured sulfate-reducing bacterium (AY251458)	95	<i>Desulfotomaculum carboxydans</i> (CP002736)	78	KT351710
	19	Uncultured prokaryote (KC107302)	84			KT351711
	20	Uncultured bacterium (FJ948567)	91	<i>Desulfosporosinus</i> sp. (AY787791)	89	KT351712
	21, 22	Uncultured bacterium (GQ200467)	85	<i>Syntrophobacter fumaroxidans</i> (CP000478)	80, 81	KT351713

fluid flow (Lueders et al. same issue). Furthermore, the release of toxic substances from SOM such as phenols (Hedges and Oades 1997, LaRowe and Van Cappellen 2011) and/or arsenic and heavy metals because of the temperature increase (Bonte et al. (2013b), might have led to the incomplete sulfate reduction as well.

The fastest sulfate depletion along the flow paths as well as the highest DNA concentration and the highest specific gene copies (approximately 6×10^7 gene copies/L, Tab. 5) indicated that the highest metabolic activity of the SRB occurred at 40 °C. Sulfate was primarily reduced in the first 13 cm of the columns. Furthermore, SRB are known to be metabolically versatile and capable of fermentation or of living a syntrophic lifestyle. Thus, they might have been metabolically active even though the TEA were depleted (Muyzer and Stams 2008, Plugge et al. 2011). Additionally, syntrophic relations between acetate-oxidizing or fermentative bacteria and hydrogenotrophic SRB might have played an important role in sulfate reduction. *S. fumaroxidans*-related species were detected at 40 °C and 70 °C, and they are known to live syntrophically in the presence of hydrogenotrophic microorganisms or to reduce sulfate (Harmsen et al. 1998, Plugge et al. 2012).

The release of sulfate from the sediment was shown in batch experiments using the same sediments and water as in the column approach (Jesubeck 2012). However, in the columns, the released sulfate was not detected in the effluent because of its rapid reduction and precipitation with iron. Kwon et al. (2014) showed that sulfide produced by SRB promoted the reduction of ferric iron and the precipitation of ferrous iron as iron sulfide. Thus, the Fe^{2+} amount observed in the effluents reflected the net result of the reductive iron dissolution and the precipitation of iron minerals. The IRB and the iron detected in the effluents as well as the mass balances also indicated an ongoing iron reduction after the sulfate reduction was running. It is assumed that micro niches developed and provided suitable living conditions for SRB and IRB that benefited from the concurrent reduction of iron and sulfate. The subsequent precipitation of iron with sulfide led to the mitigation of hydrogen sulfide toxicity. This finding is consistent with a previous study that also found a simultaneous microbial reduction of iron and sulfate in an experimental approach with sediments and fluids from the Mahomet aquifer (Flynn et al. 2013).

Methanogenic activity at 25 °C after depletion of sulfate

Methanogenic activity was observed at 25 °C after a flow-through of 140 L and this corresponded to the highest decrease in the acetate concentration. Consistently, genetic fingerprinting revealed the presence of obligate acetoclastic *Methanosaeta concilii*-like archaea in the effluents. Sequences related to *M. concilii* were also identified via the co-migrated bands of weaker intensity in the 40 °C fluids. Additionally, organisms that were distantly related to an uncultured methanogenic archaeon (93-94% similarity) were detected. Coincident with the methane formation the highest *Methanosaeta*-specific 16S rRNA gene copies were determined at 25 °C, at an average of 1×10^7 gene copies/L. Whereas three to five orders of magnitude lower numbers were observed in the 10 °C, 40 °C, and 70 °C effluents

(Tab. 5). In contrast, Bonte et al. (2013a) found the highest methane production at 40 °C. However, this methane was formed hydrogenotrophically.

Methanogenesis from acetate is primarily influenced by the acetate availability (Zinder et al. 1990), pH, temperature, salinity (van den Berg et al. 1976), redox potential (Rieger et al. 2006), sulfide, and ammonium concentrations (Chen 2008). All the columns were operated at suitable temperatures as well as under appropriate pH and salinity conditions for methanogenesis (van den Berg et al. 1976, Zinder et al. 1990).

Methanosaeta species prefer environments with low acetate concentrations (< 60 mg/L) (Zinder et al. 1990) as provided in our experiments. In addition, methane production was initiated at 25 °C after the sulfate concentration was below 4.8 mg/L along the column flow path (Jesußek et al. 2013b). This went along with a decrease in acetate concentration along the column flow path below the detection limit and a TIC increase from 7.4 mg/L to 10.4 mg/L. Methanogenesis was also observed at sulfate concentrations below 3 mg/L in intertidal sediment cores and in groundwater wells (Winfrey and Ward 1983, Flynn et al. 2013). At 10 °C, the sulfate reduction had just been initiated. Therefore the sulfate concentration was above 5 mg/L. The redox conditions were likely still unfavorable for methanogenesis and the gene copy numbers of *M. concilii* were consistently below the detection limit. *M. concilii* is described to use acetate as sole energy source for growth, and growth was observed at temperatures between 10 °C and 45 °C (Patel and Sprott 1990). However, thermophilic *Methanosaeta* strains with a temperature optima of up to 70 °C are also described (Zinder et al. 1984, Kamagata and Mikami 1991).

M. concilii-specific 16S rRNA genes were also detected at 40 °C, however, the methane was below the detection limit. Blake et al. (2015) observed methanogenic activity between 5 °C and 40 °C (optimum at 30 °C) in acetate-amended arctic sediment microcosms and concluded that the temperature was the prevailing factor in the structure and functionality of the methanogenic community. Therefore, aside from the temperature, some other sediment-specific factors influenced the methanogenic activity in our approach. As already mentioned, the CUE values of methanogens are lower than the CUE values of SRB (Widdel and Pfennig 1977, Zehnder et al. 1980). Thus, the increase in the methanogenic biomass was slower and resulted in a slow increase in the methane concentration over the sediment column flow paths. Furthermore, *Methanosaeta* species have generation times of two to 12 days (Jetten et al. 1992). Therefore, an extended adaptation phase to temperatures far above the original sediment temperature might have retarded methane formation at 40 °C. However, the microbial community did not change substantially during the three-month period of molecular biological monitoring. Thus, we speculate that a temperature-related inhibition caused by toxic substances obstructed methanogenesis at temperatures of 40 °C and above. The release of toxic substances resulting from SOM inhibiting the methanogens (Fang and Chang 1997), or arsenic, and other heavy metals (Bonte et al. 2013b) may have resulted in toxic effects for the methanogens.

Mass balances of carbon and TEA indicate similar metabolic processes in all columns

The joint evaluation of mass balances was applied as an approach to quantify the primary microbial metabolic processes in the sediment columns (Fig. 4, Fig. 5, Tab. 3) and to correlate this to the microbial abundance. The mass balances showed that aerobic OM degradation and biomass formation were among the prevailing processes at all temperatures (Fig. 5). Furthermore, sulfate reduction played a major role in almost all experiments after its initiation.

The microbial community composition corresponded to the aerobic OM degradation and the sulfate reduction found in the column effluents. Specifically, facultative anaerobic OM-degrading microorganisms as well as anaerobic SRB were determined at all temperatures. The facultative anaerobes detected in the effluents are commonly found in aquatic environments and use oxygen and/or nitrate as TEA (Dugan et al. 1992, Kalmbach et al. 1999, Reinhold-Hurek and Hurek 2000). Nitrate was available as an alternative electron acceptor only at low amounts introduced with the influents. Therefore, the detected facultative anaerobic organisms probably used oxygen for their metabolism. Aerobic bacteria were also shown as indicators for oxygen availability in fluids produced from a 1.3 km deep reservoir of a HT-ATES (Westphal et al. 2016). Assuming that the oxygen concentration in the column influents was 9.3 mg/L, aerobic degradation was a major microbial process and contributed between 37% and 58% to the acetate conversion.

Denitrification, manganese reduction, and iron reduction were observed in all the columns. However, denitrification played a minor role because of the low nitrate inflow and only between 2% and 8% of the total acetate amount was degraded because of denitrification. Furthermore, sequences affiliated with the iron-reducing genera *Thermosinus*, *Ferribacterium* and *Fervidicola*, were detected at 10 °C, 25 °C, and 70 °C. Iron was released from the sediments and partly precipitated with sulfides and hydroxides. Nevertheless, the Fe²⁺ discharge ranged between 12 and 248 mg Fe²⁺ in total, which corresponded to an acetate consumption of 1 to 13 mg C (Tab. 3: min. value). Assuming that iron precipitated with the sulfide from the sulfate reduction, the maximal [C]acetate consumption for iron reduction ranged between 13 and 100 mg C (Tab. 3: max. value). Furthermore, iron carbonate precipitation also might have played a role. However, this precipitation could not be included in the balance because the data were not available. Including the formation of FeS in the balance, this contributed to the total acetate degradation only between 6% and 12%. Notably, the calculated acetate decreases differed only slightly (between 3% and 13%) from the observed decreases at 10 °C and 25 °C. Thus, it seems that iron reduction to acetate degradation only played a minor role. This is further supported by the consistency between the calculated CO₂ increase and the observed TIC increase for the 10 °C and 25 °C experiments. The deviation of 12% to 16% is in the range of the accuracy of the balance.

From 25 °C to 70 °C, the sulfate reduction was a crucial process leading to [C]acetate consumption that were between 26% and 32% of the total amount. SRB related to *Desulfotomaculum*, *Desulfosporosinus* and *Desulfovibrio* were identified in the column fluids. Also Bonte et al. (2013a)

observed that sulfate reduction is a dominant process in sediment columns tempered to 25 °C and 60 °C. At 10 °C, sulfate reduction was initiated at the end of the balancing period (Fig. 3). Therefore, the amount of acetate consumption by sulfate reduction was negligible in the total mass balance. However, different genera of SRB and a specific gene copy number of 2×10^5 copies/L were identified in the 10 °C effluents. This finding clearly shows that the molecular biological monitoring of these effluents is a sensitive tool for observing processes already when they are just initiated. Remarkably, the methanogenesis performed by *Methanosaeta*-like acetoclastic methanogens played a major role at 25 °C only. Here, the [C]acetate and TOC decreases were within the same range and had good consistency with the sum of the TIC and [C]methane increases (Fig. 4).

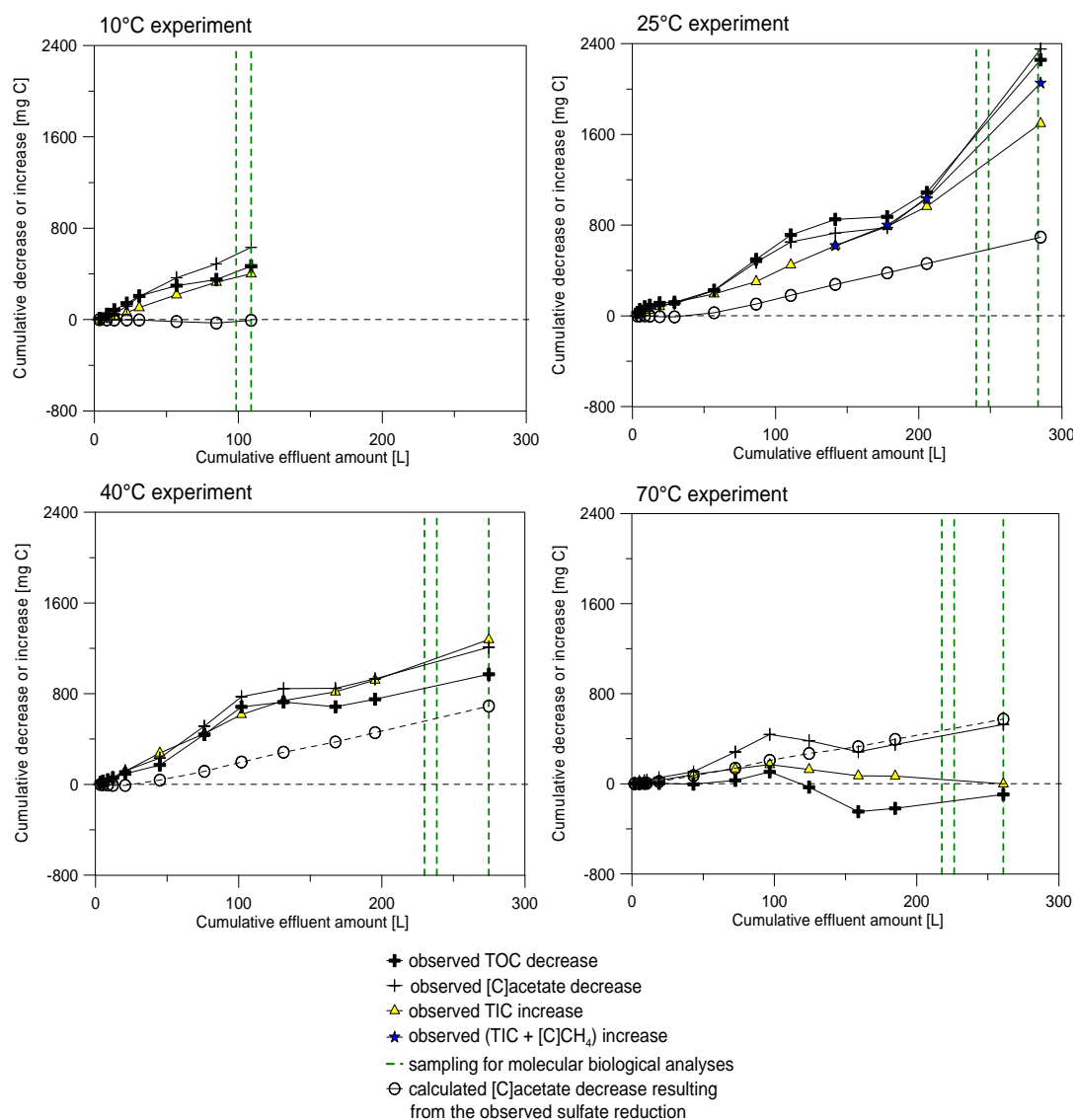


Figure 4. Cumulative amounts of the observed TOC and [C]acetate decreases, of the calculated [C]acetate decreases resulting from the observed sulfate reduction as well as of the observed TIC and [C]CH₄ increases over the cumulative effluent amount.

The [C]acetate decreases were roughly within the expected range of the calculated microbial [C]acetate consumption for the 10 °C and 25 °C columns (Fig. 5). It should be noted that the aerobic OM degradation might be overestimated because the oxygen introduction was calculated based on an oxygen concentration of 9.3 mg/L provided by the water supplier. However, the balances were conducted with these data (9.3 mg/L) and also with a lower oxygen concentration of 3 mg/L (data not shown). Hereby, the balance with an oxygen concentration 9.3 mg/L fitted better to the measured acetate decrease and TIC increase. In contrast to the good conformity of carbon balances at 10 °C and 25 °C, the observed [C]acetate decreases for the 40 °C and 70 °C columns were significantly lower than the calculated decreases with 45% and 73%, respectively. These differences reinforce the suggestion of a SOM release and its subsequent microbial degradation to CO₂ at temperatures above 40 °C.

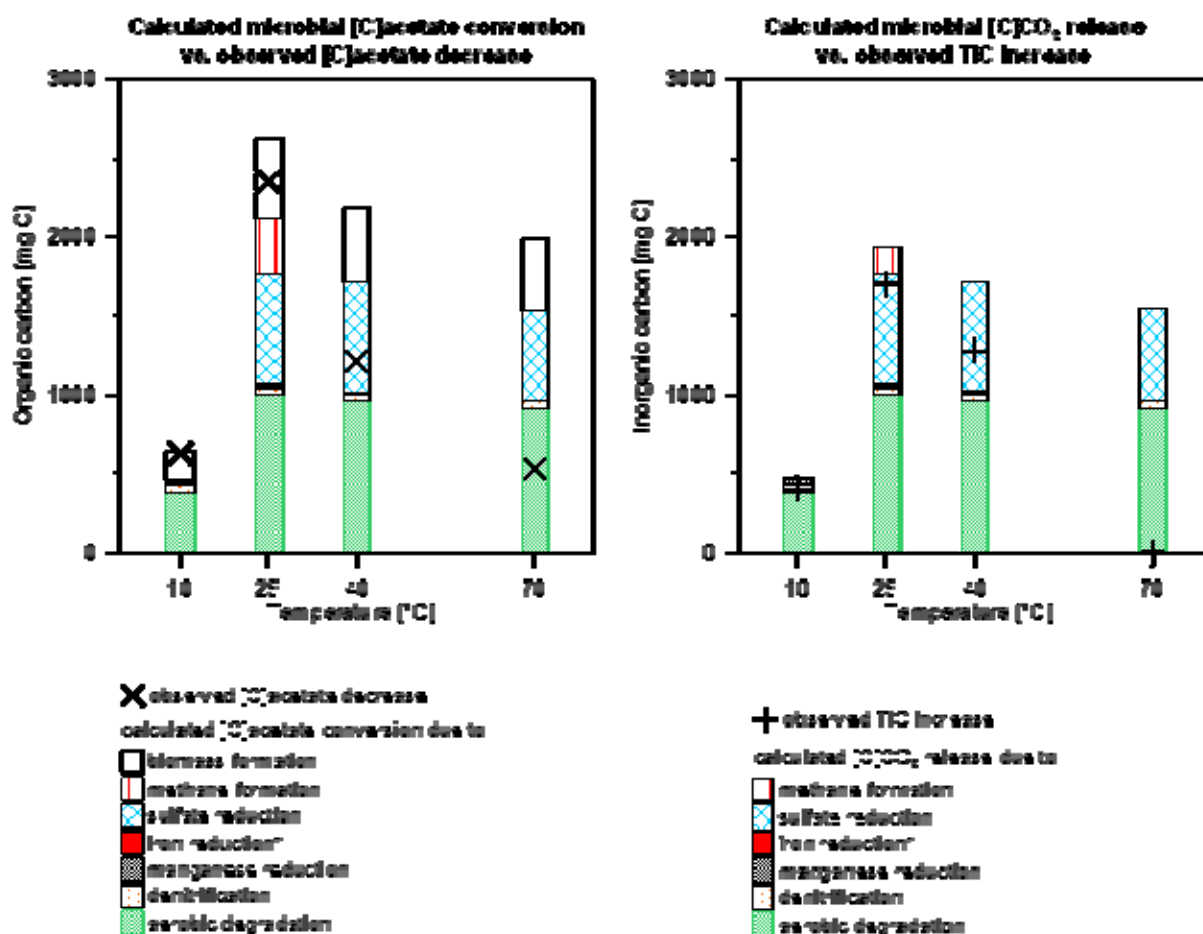


Figure 5. Organic and inorganic carbon mass balances based on changes in the fluid composition, including TEA, TOC, TIC, acetate and methane. (*) Precipitates such as FeS were not measured and thus not included in the calculation.

At 10 °C and 25 °C, the observed TIC increases were roughly consistent with the calculated ones. However, at 40 °C and above, the observed TIC was lower than the calculated TIC. This indicates CO₂ degassing at higher temperature as the solubility of CO₂ decreases by a factor of five with increasing temperatures from 10 °C to 70 °C (Carroll et al. 1991). Thus, degassing very likely reduced the TIC above 40 °C considerably. In addition, this substantiated the assumption of formed stagnation zones by trapped gases at higher temperatures. Furthermore, the precipitation of carbonates because of degassing and local pH increases might have enhanced the effect of the increasing inhomogeneity at higher temperatures in the course of the experiment. This probably led to a shorter hydraulic residence time reducing the time for microbial processes, and consequently, to a lower total sulfate reduction. Carbonate precipitations might have led to a decrease in the TIC. However, the calcium concentration did not change notably in any of the experiments, indicating that calcium carbonate precipitations might have been of lower relevance.

Even though the composition of the microbial biocenosis differed in the different tempered columns, the similar microbial conversion processes aerobic degradation (hydrolysis), fermentation and sulfate reduction dominated in the columns. Methanogenesis additionally occurred at 25 °C only. Thus, the microbial communities in each column catalyzed similar metabolic processes, although the species differed depending on the temperature. That is in accordance with *in-situ* observations of Hartog et al. (2013). They concluded that the functions of the microbial community are not significantly affected by a temperature increase because of the similar metabolic activities and capabilities of the microorganisms with different temperature optima.

In addition, the availability of TEA and the temperature were crucial for the microbial community composition in our experiments. This was also seen by Christoffersen et al. (2006) who showed that the substrate availability and temperature triggered very complex dynamics in microbial communities.

Highest Carbon Use Efficiency at 40 °C

In our study, the highest bacterial and SRB gene copy numbers were detected for the 40 °C fluids (Tab. 5), although sulfate reduction was limited by low sulfate concentrations at all temperatures. This indicated that the bacterial community as well as the SRB community had the highest CUE at 40 °C. Widdel and Pfennig (1977) as well as Zehnder et al. (1980) showed that SRB have higher CUE values than methanogens if acetate is the only carbon source. Thus, the SRB and bacterial abundance were the highest in the 40 °C effluents where the sulfate reduction activity was the highest, despite the higher acetate degradation efficiency at 25 °C. After methanogenesis was initiated at 25 °C, this column became most effective in acetate degradation, leading to acetate concentrations below the detection limit. However, the DNA concentration remained lower than in the 40 °C effluents. Different studies show that the CUE depends on the environmental conditions: substrate type, substrate availability, the microbial community composition, degradation, and assimilation pathways (Allison et al. 2010, Manzoni et al. 2012, Sinsabaugh et al. 2013, Allison 2014). A higher nutrient

availability tends to increase the CUE and a temperature increase was shown to decrease the CUE, but only temporarily (Allison et al. 2010, Frey et al. 2013). The CUE for methanogenesis is significantly lower than it is for the other TEA-consuming processes (Tab. 2). Thus, the highest acetate degradation at 25 °C influences the biomass yield to a lower extent. The greater CUE at 40 °C might have contributed to the greater biomass content in the effluents. Furthermore, the increased degradation of SOM due to a temperature-related higher availability of SOM might have led to a higher abundance in the fluid.

Conclusions

The temperature increase in columns that were filled with lignite sand from a former gravel pit, and the subsequent SOM release and/or acetate addition led to the formation of different microhabitats in the sediment columns. Due to a decrease in TEA availability, a spatio-temporal succession of microbially driven reactions developed. These reactions required different redox conditions such as aerobic OM degradation, sulfate reduction, and methanogenesis. In each column, the microbial community had similar metabolic capabilities, although the species differed depending on the temperature. This study is in accordance to other *in-situ* or similar laboratory-scale investigations observing a temperature dependent change in the microbial community composition. However, this study firstly revealed the highest bacterial diversity at a high incubation temperature of 70 °C. Whereas the microbial community composition in the effluents reflected the primary processes that occurred in the sediment columns, the microbial abundance was strongly influenced by large differences in the CUE of the specific metabolic reactions. Nevertheless, the highest gene copy numbers of *M. concilii* and SRB-specific gene copies corresponded to the methanogenic activity and the highest sulfate reduction rate. Thus, if SOM is released from the sediment, then a significant impact of geothermal energy storage on the natural microbial community and various metabolic activities, e. g., sulfate reduction, are expected in the temperature-influenced zone.

Acknowledgments

The authors wish to thank the German Ministry of Science, Economic Affairs and Transport and the University of Kiel for funding within the framework of the "GeoCITTI" project as well as the Federal Ministry of Education and Research for funding the "ANGUS+" (03EK3022D) project. Furthermore, we thank the Applied Geology-Hydrogeology and Engineering Geology groups from Kiel University for their support with the sampling. Also we thank the anonymous reviewer for the valuable comments to improve this manuscript.

References

- Adinolfi M, Koch M, Ruck W (1994) Ökologische und mikrobielle Folgen der Wärmespeicherung im Aquifer. *Stuttgarter Berichte zur Siedlungswasserwirtschaft* 124:89–106
- Alfreider A, Krossbacher M, Psenner R (1997) Groundwater samples do not reflect bacterial densities and activity in subsurface systems. *Water Res* 31:832–840
- Allison SD (2014) Modeling adaptation of carbon use efficiency in microbial communities. *Front Microbiol* 5:1–9
- Allison SD, Wallenstein MD, Bradford MA (2010) Soil-carbon response to warming dependent on microbial physiology. *Nat Geosci* 3:336–340
- Altschul S, Gish W, Miller W (1990) Basic local alignment search tool. *J Mol Biol* 215:403–410
- Amann RI, Stromley J, Devereux R, Key R, Stahl DA (1992) Molecular and microscopic identification of sulfate-reducing bacteria in multispecies biofilms. *Appl Environ Microbiol* 58:614–623
- Anderson JM (1973) Carbon dioxide evolution from two temperate, deciduous woodland soils. *J Appl Ecol* 10:361–378
- Apple JK, del Giorgio PA, Kemp WM (2006) Temperature regulation of bacterial production, respiration, and growth efficiency in a temperate salt-marsh estuary. *Aquat Microb Ecol* 43:243–254
- Arning E, Kölling M, Schulz HD, Panteleit B, Reichling J (2006) Einfluss oberflächennaher Wärmegewinnung auf geochemische Prozesse im Grundwasserleiter. *Grundwasser* 11:27–39
- Barton LL, Fauque GD (2009) Biochemistry, physiology and biotechnology of sulfate-reducing bacteria. *Adv Appl Microbiol* 68:41–48
- Bauer S, Beyer C, Dethlefsen F, Dietrich P, Duttmann R, Ebert M, Feeser V, Görke U, Köber R, Kolditz O, Rabbel W, Schanz T, Schäfer D, Würdemann H, Dahmke A (2013) Impacts of the use of the geological subsurface for energy storage: an investigation concept. *Environ Earth Sci* 70:3935–3943
- Blake LI, Tveit A, Øvreås L, Head IM, Gray ND (2015) Response of methanogens in arctic sediments to temperature and methanogenic substrate availability. *PLoS ONE* 10:e0129733
- Bonte M, Stuyfzand PJ, Hulsmann A, Van Beelen P (2011a) Underground thermal energy storage: environmental risks and policy developments in the Netherlands and European Union. *Ecol Soc* 16:22–37
- Bonte M, Stuyfzand PJ, van den Berg GA, Hijnen WAM (2011b) Effects of aquifer thermal energy storage on groundwater quality and the consequences for drinking water production: a case study from the Netherlands. *Water Sci, Technol*, p 63
- Bonte M, Röling WFM, Zaura E, van der Wielen PWJJ, Stuyfzand PJ, van Breukelen BM (2013a) Impacts of shallow geothermal energy production on redox processes and microbial communities. *Environ Sci Technol* 47:14476–14484
- Bonte M, van Breukelen BM, Stuyfzand PJ (2013b) Temperature-induced impacts on groundwater quality and arsenic mobility in anoxic aquifer sediments used for both drinking water and shallow geothermal energy production. *Water Res* 47:5088–5100
- Brielmann H, Griebler C, Schmidt SI, Michel R, Lueders T (2009) Effects of thermal energy discharge on shallow groundwater ecosystems. *FEMS Microbiol Ecol* 68:273–286
- Brielmann H, Lueders T, Schreglmann K, Ferraro F, Avramov M, Hammerl V, Blum P, Bayer P, Griebler C (2011) Oberflächennahe Geothermie und ihre potenziellen Auswirkungen auf Grundwasserökosysteme. *Grundwasser* 16:77–91

- Brons HJ, Griffioen J, Appelo CAJ, Zehnder AJB (1991) (Bio)geochemical reactions in aquifer material from a thermal energy storage site. *Water Res* 25:729–736
- Campbell IL, Postgate JR (1965) Classification of the spore-forming sulfate-reducing bacteria. *Bacteriol Rev* 29:359–363
- Carroll JJ, Slupsky JD, Mather AE (1991) The solubility of carbon dioxide in water at low pressure. *J Phys Chem Ref Data* 20(6):1201–1209
- Chapelle FH (2000) The significance of microbial processes in hydrogeology and geochemistry. *Hydrogeol J* 8:41–46
- Chen Y, Cheng JJ, Creamer KS (2008) Inhibition of anaerobic digestion process: a review. *Bioresour Technol* 99:4044–4064
- Christoffersen K, Andersen N, Søndergaard M, Liboriussen L, Jeppesen E (2006) Implications of climate-enforced temperature increases on freshwater pico- and nanoplankton populations studied in artificial ponds during 16 months. *Hydrobiologia* 560:259–266
- Dachroth WR (2002) *Handbuch der Baugeologie und Geotechnik*. Springer, Berlin, Heidelberg
- Daumas S, Cord-Ruwisch R, Garcia JL (1988) *Desulfotomaculum geothermicum* sp. nov., a thermophilic, fatty acid-degrading, sulfate-reducing bacterium isolated with H₂ from geothermal ground water. *Antonie Van Leeuwenhoek* 54:165–178
- De Rezende JR, Kjeldsen KU, Hubert C, Finster K (2013) Dispersal of thermophilic *Desulfotomaculum* endospores into Baltic Sea sediments over thousands of years. *ISME J* 7:72–84
- Dugan PR, Stoner DL, Pickrum HM (1992) The genus *Zoogloea*. In: Balows A, Trüper HG, Dworkin M, Harder W, Schleifer K-H (eds) *The prokaryotes*. Springer, New York, pp 3952–3964
- Eugster WJ, Sanner B (2007) Technological status of shallow geothermal energy in Europe. Paper presented at the proceedings European geothermal congress, Unterhaching, Germany, 1–8 June 2007
- Fang HHP, Chan O (1997) Toxicity of phenol towards anaerobic biogranules. *Water Res* 31:2229–2242
- Fardeau M-L, Barsotti V, Cayol J-L, Guasco S, Michotey V, Joseph M, Bonin P, Ollivier B (2010) *Caldinitratiruptor microaerophilus*, gen. nov., sp. nov. isolated from a French hot spring (Chaudes-Aigues, Massif Central): a novel cultivated facultative microaerophilic anaerobic thermophile pertaining to the *Symbiobacterium* branch within the Firmicutes. *Extremophiles* 14:241–247
- Flynn TM, Sanford RA, Ryu H, Bethke CM, Levine AD, Ashbolt NJ, Santo Domingo JW (2013) Functional microbial diversity explains groundwater chemistry in a pristine aquifer. *BMC Microbiol* 13:146
- Frey SD, Lee J, Melillo JM, Six J (2013) The temperature response of soil microbial efficiency and its feedback to climate. *Nat Clim Chang* 3:395–398
- Gafan GP, Lucas VS, Roberts GJ, Wilson M, Spratt DA, Petrie A (2005) Statistical analyses of complex denaturing gradient gel electrophoresis profiles. *J Clin Microbiol* 43:3971–3978
- Geets J, Borremans B, Vangronsveld J, Diels L, Van Der Lelie D (2005) Molecular monitoring of SRB community structure and dynamics in batch experiments to examine the applicability of in situ precipitation of heavy metals for groundwater remediation. *J Soils Sediments* 5:149–163
- Geets J, Borremans B, Diels L, Springael D, Vangronsveld J, van der Lelie D, Vanbroekhoven K (2006) DsrB gene-based DGGE for community and diversity surveys of sulfate-reducing bacteria. *J Microbiol Methods* 66:194–205
- Gödde M, David MB, Christ MJ, Kaupenjohann M, Vance GF (1996) Carbon mobilization from the forest floor under red spruce in the northeastern U.S.A. *Soil Biol Biochem* 28:1181–1189

- Griebler C, Mindl B, Slezak D, Geiger-Kaiser M (2002) Distribution patterns of attached and suspended bacteria in pristine and contaminated shallow aquifers studied with an in situ sediment exposure microcosm. *Aquat Microb Ecol* 28:117–129
- Hähnlein S, Bayer P, Ferguson G, Blum P (2013) Sustainability and policy for the thermal use of shallow geothermal energy. *Energy Policy* 59:914–925
- Harmsen HJM, Van Kuijk BLM, Plugge CM, Akkermans ADL, De Vos WM, Stams AJM (1998) *Syntrophobacter furnaroxidans* sp. nov., a syntrophic propionate-degrading sulfate-reducing bacterium. *Int J Syst Bacteriol* 48:1383–1388
- Hartog N, Drijver B, Dinkla I, Bonte M (2013) Field assessment of the impacts of Aquifer Thermal Energy Storage (ATES) systems on chemical and microbial groundwater composition. *Eur. Geotherm. Congr.* 2013 Pisa, Italy, 3–7 June 2013. pp 1–8
- Hedges JJ, Oades JM (1997) Comparative organic geochemistries of soils and marine sediments. *Org Geochem* 27:319–361
- Hekmat, MA (1982). Sedimentologie, Petrographie und Geochemie des Miozäns aus den Bohrungen Osdorf – westlich von Hamburg, Neu-Börnsen und Kasseburg im süd-östlichen Schleswig-Holstein. Thesis. University of Hamburg
- Henze M (2008) Biological wastewater treatment: principles, modelling and design. IWA publishing, London
- Hubert C, Loy A, Nickel M, Arnosti C, Baranyi C, Brüchert V, Ferdelman T, Finster K, Christensen FM, de Rezende JR, Vandieken V, Jørgensen BB (2009) A constant flux of diverse thermophilic bacteria into the cold Arctic seabed. *Science*(80-) 325:1541–1544
- Isaksen MF, Bak F, Jørgensen BB (1994) Thermophilic sulfate-reducing bacteria in cold marine sediment. *FEMS Microbiol Ecol* 14:1–8
- Jesußek A (2012) Temperaturbedingte Auswirkungen unterirdischer Wärmespeicherung auf hydrogeochemische Sediment-Wasser-Wechselwirkungen in einem oberflächennahen Grundwasserleiter, Dissertation, Universität Kiel
- Jesußek A, Grandel S, Dahmke A (2013a) Impacts of subsurface heat storage on aquifer hydrogeochemistry. *Environ Earth Sci* 69:1999–2012
- Jesußek A, Köber R, Grandel S, Dahmke A (2013b) Aquifer heat storage: sulphate reduction with acetate at increased temperatures. *Environ Earth Sci* 69:1763–1771
- Jetten MSM, Stams AJM, Alexander JBZ (1992) Methanogenesis from acetate: a comparison of the acetate metabolism in *Methanothrix soehngenii* and *Methanosarcina* spp. *FEMS Microbiol Rev* 88:181–198
- Joannis-Cassan C, Delia M-L, Riba J-P (2007) Biofilm growth kinetics on hydrocarbon in a porous medium under biostimulation conditions. *Environ Progr* 26(2):140–148
- Kabuth A, Dahmke A, Beyer C, Dethlefsen F, Dietrich P, Duttmann R, Ebert M, Feeser V, Görke U, Köber R, Kolditz O, Rabbel W, Schanz T, Schäfer D, Würdemann H, Bauer S (same issue) Energy storage in the geological subsurface: dimensioning, risk analysis and spatial planning–The ANGUS + project. Submitted to *Environ Earth Sci*
- Kalmbach S, Manz W, Wecke J, Szewzyk U (1999) *Aquabacterium* gen. nov., with description of *Aquabacterium citratiphilum* sp. nov., *Aquabacterium parvum* sp. nov. and *Aquabacterium commune* sp. nov., three in situ dominant bacterial species from the Berlin drinking water system. *Int J Syst Bacteriol* 49:769–777
- Kamagata Y, Mikami E (1991) Isolation and characterization of a novel thermophilic *Methanosaeta* strain. *Int J Syst Bacteriol* 41:191–196

- Klein W, Bordeau P P (1989) Mobility of environmental chemicals, including abiotic degradation. In: Haines JA, Klein W, Krishna Murti CR (eds) *Ecotoxicol Climate*. Wiley, Chichester, pp 65–78
- Kwon MJ, Boyanov MI, Antonopoulos DA, Brulc JM, Johnston ER, Skinner KA, Kemner KM, O'Loughlin EJ (2014) Effects of dissimilatory sulfate reduction on FeIII (hydr)oxide reduction and microbial community development. *Geochim Cosmochim Acta* 129:177–190
- Lane D (1991) 16S/23S rRNA sequencing. In: Stackebrandt E, Goodfellow M (eds) *Nucleic Acid Tech. Bact. Syst.* John Wiley and Son, New York, pp 115–175
- LaRowe DE, Van Cappellen P (2011) Degradation of natural organic matter: a thermodynamic analysis. *Geochim Cosmochim Acta* 75:2030–2042
- Lee KS (2013) *Underground thermal energy storage*. Springer, London
- Lerm S, Alawi M, Miethling-Graff R, Wolfgramm M, Rauppach K, Seibt A, Würdemann H (2011a) Influence of microbial processes on the operation of a cold store in a shallow aquifer: impact on well injectivity and filter lifetime. *Grundwasser* 16:93–104
- Lerm S, Alawi M, Miethling-Graff R, Seibt A, Wolfgramm M, Rauppach K, Würdemann H (2011b) Mikrobiologisches Monitoring in zwei geothermisch genutzten Aquiferen des Norddeutschen Beckens. Microbiological monitoring of two geothermally used aquifers in the North German Basin. *Zeitschrift für Geol Wissenschaften* 39:195–212
- Lerm S, Westphal A, Miethling-Graff R, Alawi M, Seibt A, Wolfgramm M, Würdemann H (2013) Thermal effects on microbial composition and microbiologically induced corrosion and mineral precipitation affecting operation of a geothermal plant in a deep saline aquifer. *Extremophiles* 17:311–327
- Lienen T, Lüders K, Halm H, Westphal A, Köber R, Würdemann H (same issue) Effects of geothermal usage on shallow aerobic aquifer systems - Temporary increase in abundance and activity of sulfate reducing and sulfur oxidizing bacteria. Submitted to *Environ Earth Sci*
- Lovley DR, Phillips EJ (1988) Novel mode of microbial energy metabolism: organic carbon oxidation coupled to dissimilatory reduction of iron or manganese. *Appl Environ Microbiol* 54:1472–1480
- Lueders K, Koeber R, Dahmke A (same issue) Formation of gas phases in context of thermal energy storage in shallow aquifers. Submitted to *Environ Earth Sci*
- Manzoni S, Taylor P, Richter A, Porporato A, Ågren GI (2012) Environmental and stoichiometric controls on microbial carbon-use efficiency in soils. *New Phytol* 196:79–91
- McCoy WF, Olson BH (1985) Fluorometric determination of the DNA concentration in municipal drinking water. *Appl Environ Microbiol* 49:811–821
- Mori K, Hanada S, Maruyama A, Marumo K (2002) *Thermanaeromonas toyohensis* gen. nov., sp. nov., a novel thermophilic anaerobe isolated from subterranean vein in the Toyoha Mines. *Int J Syst Evol Microbiol* 52:1675–1680
- Muyzer G, Stams AJM (2008) The ecology and biotechnology of sulphate-reducing bacteria. *Nat Rev Microbiol* 6:441–454
- Muyzer G, de Waal EC, Uitterlinden AG (1993) Profiling of complex microbial populations by denaturing gradient gel electrophoresis analysis of polymerase chain reaction-amplified genes coding for 16S rRNA. *Appl Environ Microbiol* 59:695–700
- Nadkarni MA, Martin FE, Jacques NA, Hunter N (2002) Determination of bacterial load by real-time PCR using a broad-range (universal) probe and primers set. *Microbiology* 148:257–266
- Ogg CD, Patel BKC (2009) *Fervidicola ferrireducens* gen. nov., sp. nov., a thermophilic anaerobic bacterium from geothermal waters of the Great Artesian Basin, Australia. *Int J Syst Evol Microbiol* 59:1100–1107

- Ollivier B, Cord-Ruwisch R, Hatchikian EC, Garcia JL (1988) Characterization of *Desulfovibrio fructosovorans* sp. nov. Arch Microbiol 149:447–450
- Parkes RJ, Gibson GR, Mueller-Harvey I, Buckingham WJ, Herbert RA (1989) Determination of the substrates for sulphate-reducing bacteria within marine and estuarine sediments with different rates of sulphate reduction. J Gen Microbiol 135:175–187
- Parshina SN, Sipma J, Nakashimada Y, Henstra AM, Smidt H, Lysenko AM, Lens PNL, Lettinga G, Stams AJM (2005) *Desulfotomaculum carboxydivorans* sp. nov., a novel sulfate-reducing bacterium capable of growth at 100% CO. Int J Syst Evol Microbiol 55:2159–2165
- Patel GB, Sprott GD (1990) *Methanosaeta concilii* gen. nov. sp. nov. (“*Methanothrix concilii*”) and *Methanosaeta thermoacetophila* nom. rev., comb. nov. Int J Syst Bacteriol 82:79–82
- Pedersen K, Arlinger J, Eriksson S, Hallbeck A, Hallbeck L, Johansson J (2008) Numbers, biomass and cultivable diversity of microbial populations relate to depth and borehole-specific conditions in groundwater from depths of 4–450 m in Olkiluoto, Finland. ISME J 2:760–775
- Pfennig N, Widdel F, Trüper HG (1981) The dissimilatory sulfate-reducing bacteria. In: Starr MP, Stolp H, Trüper HG, Balows A, Schlegel HG (eds) The prokaryotes, vol I. Springer, Berlin Heidelberg, pp 926–940
- Plugge CM, Zhang W, Scholten JCM, Stams AJM (2011) Metabolic flexibility of sulfate-reducing bacteria. Front Microbiol 2:1–8
- Plugge CM, Henstra AM, Worm P, Swarts DC, Paulitsch-Fuchs AH, Scholten JCM, Lykidis A, Lapidus AL, Goltsman E, Kim E, McDonald E, Rohlin L, Crable BR, Gunsalus RP, Stams AJM, McInerney MJ (2012) Complete genome sequence of *Syntrophobacter fumaroxidans* strain (MPOBT). Stand Genom Sci 7:91–106
- Poli A, Esposito E, Lama L, Orlando P, Nicolaus G, de Appolonia F, Gambacorta A, Nicolaus B (2006) *Anoxybacillus amylolyticus* sp. nov., a thermophilic amylase producing bacterium isolated from Mount Rittmann (Antarctica). Syst Appl Microbiol 29:300–307
- Rabus R, Hansen T, Widdel F (2006) Dissimilatory sulfate- and sulfur-reducing prokaryotes. In: Dworkin M, Falkow S, Rosenberg E, Schleifer K-H, Stackebrandt E (eds) prokaryotes, vol 2. Springer, New York, pp 659–768
- Reimann C, Garrett RG (2005) Geochemical background—concept and reality. Sci Total Environ 350:12–27
- Reinhold-Hurek B, Hurek T (2000) Reassessment of the taxonomic structure of the diazotrophic genus *Azoarcus* sensu lato and description of three new genera and new species, *Azovibrio restrictus* gen. nov., sp. nov., *Azospira oryzae* gen. nov., sp. nov. and *Azonexus fungiphilus* gen. nov., sp. nov. Int J Syst Evol Microbiol 2:649–659
- Rieger C, Weiland P (2006) Prozessstörungen frühzeitig erkennen. Forschung und Praxis 4:18–20
- Robador A, Brüchert V, Jørgensen BB (2009) The impact of temperature change on the activity and community composition of sulfate-reducing bacteria in arctic versus temperate marine sediments. Environ Microbiol 11:1692–1703
- Sand W (2003) Microbial life in geothermal waters. Geothermics 32:655–667
- Sawayama S, Tada C, Tsukahara K, Yagishita T (2004) Effect of ammonium addition on methanogenic community in a fluidized bed anaerobic digestion. J Biosci Bioeng 97:65–70
- Schippers A, Reichling J (2006) Laboruntersuchungen zum Einfluss von Temperaturveränderungen auf die Mikrobiologie des Untergrundes. Grundwasser 11:40–45

- Shigematsu T, Tang Y, Kawaguchi H, Ninomiya K, Kijima J, Kobayashi T, Morimura S, Kida K (2003) Effect of dilution rate on structure of a mesophilic acetate-degrading methanogenic community during continuous cultivation. *J Biosci Bioeng* 96:547–558
- Sinsabaugh RL, Manzoni S, Moorhead DL, Richter A (2013) Carbon use efficiency of microbial communities: stoichiometry, methodology and modelling. *Ecol Lett* 16:930–939
- Sørensen J, Christensen D, Jørgensen BB (1981) Volatile fatty acids and hydrogen as substrates for sulfate-reducing bacteria in anaerobic marine sediment. *Appl Environ Microbiol* 42(1):5–11
- Sowers L, York KP, Stiles L (2006) Impact of thermal buildup on groundwater chemistry and aquifer microbes. 10th International conference on thermal storage, Ecostock, USA, pp 1–7
- Stackebrandt E, Sproer C, Rainey FA, Burghardt J, Päuker O, Hippe H (1997) Phylogenetic analysis of the genus *Desulfotomaculum*: evidence for the misclassification of *Desulfotomaculum guttoideum* and description of *Desulfotomaculum orientis* as *Desulfosporosinus orientis* gen. nov., comb. nov. *Int J Syst Bacteriol* 47:1134–1139
- Stadtwerke Kiel (2014) Personal communication
- Stevenson B, Drilling H, Lawson P, Duncan K, Parisi V, Sufklita J (2011) Microbial communities in bulk fluids and biofilms of an oil facility have similar composition but different structure. *Environ Microbiol* 13:1078–1090
- Stoodley P, Dodds I, De Beer D, Lappin-Scott HM, Boyle JD (2005) Flowing biofilms as a transport mechanism for biomass through porous media under laminar and turbulent conditions in a laboratory reactor system. *Biofouling* 21:161–168
- Takai K, Horikoshi K (2000) Rapid detection and quantification of members of the archaeal community by quantitative PCR using fluorogenic probes. *Appl Environ Microbiol* 66:5066–5072
- Thauer RK, Möller-Zinkhan D, Spormann aM (1989) Biochemistry of acetate catabolism in anaerobic chemotrophic bacteria. *Annu Rev Microbiol* 43:43–67
- Van Beek C (1989) Rehabilitation of clogged discharge wells in the Netherlands. *Q J Eng Geol* 22:75–80
- Van den Berg L, Patel G, Clark D, Lentz C (1976) Factors affecting rate of methane formation from acetic acid by enriched methanogenic cultures. *Can J Microbiol* 22:1312–1319
- Van Loosdrecht MCM, Eikelboom D, Gjaltema A, Mulder A, Tjihuis L, Heijnen J (1995) Biofilm structures. *Water Sci Technol* 32:35–43
- Videla HA, Characklis WG (1992) Biofouling and microbially influenced corrosion. *Int Biodeterior Biodegrad* 29:195–212
- Wagner M, Roger AJ, Flax JL, Brusseau GA, Stahl DA (1998) Phylogeny of dissimilatory sulfite reductases supports an early origin of sulfate respiration. *J Bacteriol* 180:2975–2982
- Wang Q, Garrity GM, Tiedje JM, Cole JR (2007) Naive Bayesian classifier for rapid assignment of rRNA sequences into the new bacterial taxonomy. *Appl Environ Microbiol* 73:5261–5267
- Westphal A, Lerm S, Miethling-Graff R, Seibt A, Wolfgramm M, Würdemann H (2016) Effects of plant downtime on the microbial community composition in the highly saline brine of a geothermal plant in the North German Basin. *Appl Microbiol Biotechnol* 100:3277–3290
- Whitman WB, Coleman DC, Wiebe WJ (1998) Prokaryotes: the unseen majority. *Proc Natl Acad Sci USA* 95:6578–6583
- Widdel F (1980) Anaerober Abbau von Fettsäuren und Benzoesäure durch neu isolierte Arten Sulfat-reduzierender Bakterien. Doctoral thesis, University of Göttingen

- Widdel F, Pfennig N (1977) A new anaerobic, sporing, acetate-oxidizing, sulfate-reducing bacterium, *Desulfotomaculum* (emend.) *acetoxidans*. Arch Microbiol 112:119–122
- Widdel F, Pfennig N (1981) Studies on dissimilatory sulfate-reducing bacteria that decompose fatty acids. Isolation of new sulfate-reducing bacteria enriched with acetate from saline environments. Description of *Desulfobacter postgatei* gen. nov., sp. nov. Arch Microbiol 129:395–400
- Widdel F, Pfennig N (1984) Dissimilatory sulfate- or sulfur-reducing bacteria. In: Krieg NR, Holt JG (eds) Bergey's manual of systematic bacteriology, vol 1. Williams & Wilkins, Baltimore London, pp 663–679
- Wilms R, Sass H, Köpke B, Cypionka H, Engelen B (2007) Methane and sulfate profiles within the subsurface of a tidal flat are reflected by the distribution of sulfate-reducing bacteria and methanogenic archaea. FEMS Microbiol Ecol 59:611–621
- Winfrey MR, Ward DM (1983) Substrates for sulfate reduction and methane production in intertidal sediments. Appl Environ Microbiol 45:193–199
- Würdemann H, Westphal A, Lerm S, Miethling-Graff R, Teitz S, Kasina M, Seibt A, Wolfgramm M, Eichinger F, Kleyböcker A (2016) Einfluss mikrobieller Stoffwechselprozesse auf den Betrieb geothermischer Anlagen—Analyse von Prozessstörungen und Bewertung von Gegenmaßnahmen. Groundwater 21:93–106
- York KP, Jahangir ZMGS, Solomon T, Stafford L (1998) Effects of a large scale geothermal heat pump installation on aquifer microbiota. 2nd International geothermal conference, Stockholm, pp 1–8
- Zavarzina D, Tourova T, Kuznetsov B, Bonch-Osmolovskaya E, Slobodkin A (2002) *Thermovenabulum ferriorganovorum* gen. nov., sp. nov., a novel thermophilic, anaerobic, endospore-forming bacterium. Int J Syst Evol Microbiol 52:1737–1743
- Zehnder AJB, Huser BA, Brock TD, Wuhrmann K (1980) Characterization of an acetate-decarboxylating, non-hydrogen-oxidizing methane bacterium. Arch Microbiol 124:1–11
- Zinder SH (1990) Conversion of acetic acid to methane by thermophiles. FEMS Microbiol Rev 75:125–137
- Zinder SH, Anguish T, Cardwell SC (1984) Effects of temperature on methanogenesis in a thermophilic (58°C) anaerobic digester. Appl Environ Microbiol 47:808–813